Journal of Environmental Management 405 (2026) 129635

Contents lists available at ScienceDirect

Journal of Environmental Management

journal homepage: www.elsevier.com/locate/jenvman

Research article

Long-term phycoremediation of hydroponic drainwater in a pilot-scale turbidostat

Emren Borhan, Ville Korhonen, Sema Sirin *, Yagut Allahverdiyeva **

Molecular Plant Biology, Department of Life Technologies, University of Turku, FI-20014, Turku, Finland

ARTICLE INFO

Keywords:
Greenhouse drainwater
Microalgae
Phycoremediation
Continuous cultivation
Discharge compliance
Turbidostat

ABSTRACT

Drainwater from hydroponic greenhouse production presents environmental and regulatory challenges for discharge due to high concentrations of nitrogen and phosphorus. Microalgae-based treatment (phycoremediation) has been proposed as an integrated solution to recover nutrients and mitigate effluent impact, but its long-term performance under seasonally variable, low-irradiance greenhouse conditions remains to be evaluated.

Here we report the performance of continuous phycoremediation using green microalgae *Scenedesmus* sp. NIVA-CHL 99 cultivated in 1000 L closed tubular vertical photobioreactor (PBR) treating commercial cucumber greenhouse effluent ($N–NO_3$: 233–422 mg L^{-1}; $P–PO_4$: 21–49.5 mg L^{-1}). Sixteen operations were conducted over one year (April 2024 – May 2025) under batch, chemostat, and turbidostat modes with varied hydraulic retention times (HRT: 5–20 days [d]) and solids retention times (SRT: 2.5–5 d) in Nordic greenhouse environment.

Turbidostat operation at an intermediate OD setpoint (OD_{890} = 1.2) resulted in most effective overall performance, achieving robust nitrate removal (26.1 mg $N–NO_3$ L^{-1} d^{-1}) and biomass productivity (0.55 g DW L^{-1} d^{-1}), while consistently meeting European Union (EU) discharge limits (TN < 6 mg L^{-1}; TP < 0.5 mg L^{-1}). Low-OD (OD_{890} = 0.9) turbidostat reached 41.1 mg $N–NO_3$ L^{-1} d^{-1} but compromised discharge quality. Chemostat modes yielded high biomass productivity (0.68 g DW L^{-1} d^{-1}) with less treatment flexibility. Light, temperature, and HRT/SRT effects on daily nutrient removal and biomass productivity were evaluated.

This study demonstrates the operational balance of greenhouse-integrative phycoremediation between drainwater treatment capacity, discharge compliance, and biomass productivity. Continuous turbidostat phycoremediation combines nutrient recovery with stable algal biomass production, reducing reliance on synthetic fertilizers and lowering operational costs. The approach advances year-round, scalable microalgal cultivation in the Nordics while transforming drainwater into resource stream within circular bioeconomy framework.

1. Introduction

Agricultural activities are intensifying to meet global food supply, yet nitrogen (N) and phosphorus (P) inputs often surpass crop demand (Liu et al., 2025). Excessive nutrients are continuously transferred from agricultural facilities to receiving waters, creating high nutrient loads that impair freshwater and marine ecosystems (Withers et al., 2014). As agriculture dominates global freshwater withdrawals, nutrient pollution remains a core environmental burden of modern food production (Carpenter et al., 1998; Wu et al., 2022). Mitigation strategies for agricultural run-off remain a persistent challenge in both open-field and controlled production, particularly under increasing climate variability (Juncal et al., 2023).

Controlled-environment hydroponic greenhouses support stable yields and improved resource utilization, yet soilless greenhouse cultivation generates nutrient-rich drainage streams that require treatment before safe discharge (Grewal et al., 2011; Benke and Tomkins, 2017). As greenhouse-based food production expands, effective drainwater management becomes both a regulatory necessity and an achievable goal through biotechnological solutions that combine environmental protection with sectoral feasibility (Tong et al., 2024). EU wastewater policy is progressively moving toward stricter nutrient discharge expectations, with lower N and P thresholds discussed to protect sensitive water bodies (Halleux, 2024). The regulations act as a

* Corresponding author
** Corresponding author. Department of Life Technologies, University of Turku, Tykistökatu 6A, 20520, Turku, Finland
E-mail addresses: sesiri@utu.fi (S. Sirin), allahve@utu.fi (Y. Allahverdiyeva).

https://doi.org/10.1016/j.jenvman.2026.129635
Received 18 February 2026; Received in revised form 3 April 2026; Accepted 7 April 2026
Available online 10 April 2026
0301-4797/© 2026 The Authors. Published by Elsevier Ltd. This is an open access article under the CC BY license (http://creativecommons.org/licenses/by/4.0/).

technology-driven pressure, while greenhouse effluents remain poorly suited for centralized treatment due to their inorganic dominated characteristics and continuous generation (Park et al., 2011; Mielcarek et al., 2024).

In response, microalgae-based bioremediation has been applied for agricultural and wastewater nutrient removal for several decades, though its broader industrial relevance is still being established (Li et al., 2019; Najar-Almanzor et al., 2023). Microalgae are photosynthetic microorganisms capable of nutrient removal under autotrophic conditions without external organic carbon (Goh et al., 2022; Amaro et al., 2023). Microalgal cultivation can be deployed on non-arable land and using wastewater, reducing dependence on freshwater while delivering high areal productivity (Nguyen et al., 2022; Geng et al., 2025). In greenhouse-integrated phycoremediation, industrial symbiosis is achieved through direct nutrient recycling, where drainwater serves as the growth medium and cultivation is embedded within existing infrastructure (Hultberg et al., 2013; Nagarajan et al., 2020). Life-cycle assessments indicate that microalgae systems can achieve lower greenhouse gas emissions than conventional cultivation when integrated with wastewater treatment and existing energy streams (Abdelfattah et al., 2023; Xu et al., 2024). Such systems align with the EU Green Deal and the EU Circular Economy Action Plan by coupling nutrient removal with the generation of biomass (European Commission, 2020a, 2020b).

Most phycoremediation studies are conducted at laboratory scale, over short timeframes, using batch operation, fixed environmental conditions, or synthetic media (Park et al., 2011; Mohsenpour et al., 2021; You et al., 2022). While these provide valuable mechanistic understanding and proof-of-concept validation, how phycoremediation responds to dynamically changing light, temperature, and inflow regimes, which are characteristics of practical treatment systems, remains to be fully elucidated (Sutherland et al., 2018; Arashiro et al., 2022; Sánchez-Contreras et al., 2021; Shayesteh et al., 2022). Consequently, long-term pilot-scale investigations employing real agricultural drainwater under continuous operation (chemostat or turbidostat) are scarce, leaving critical questions regarding sustained process stability, metabolic plasticity and discharge quality unanswered (Velásquez-Orta et al., 2024). In particular, the influence of upstream process configurations, including retention-time management, nutrient inflow control through dilution and recirculation, and response to diurnal and seasonal meteorological variability, has not been sufficiently resolved for robust drainwater treatment and biomass productivity under realistic seasonal variability (Chathurika et al., 2022). Addressing these gaps requires state-of-the-art biotechnological tools to monitor culture parameters and adjust upstream conditions under multi-variable culture and ambient dynamics (Pataro et al., 2023; Nordio et al., 2024).

Greenhouse cultivation is essential in the Nordic region, where short growing seasons and limited outdoor irradiance necessitate protected year-round farming systems (Unc et al., 2021). Compared with central and southern Europe, Nordic greenhouse operation is characterized by prolonged low-light periods, strong seasonal variability in irradiance, and higher demands for thermal and energy management, which together impose stricter constraints on photosynthetic cultivation processes (Katzin et al., 2021; Wacker et al., 2022). Many hydroponic greenhouse effluents are nutrient-rich and subject to increasingly stringent water-protection and discharge-control frameworks across the Nordic region, as nitrogen and phosphorus losses significantly contribute to the eutrophication of sensitive receiving waters. This regulatory pressure is reflected in Sweden, where legislation imposes a total phosphorus (TP) limit of 0.5 mg L^{-1} together with restrictive biochemical oxygen demand (BOD) thresholds (Preisner et al., 2020). Similarly, in Finland, environmental permits in sensitive catchment areas may require TP concentrations as low as 0.1-0.3 mg L^{-1} to support the achievement of Good Environmental Status (GES) in the Baltic Sea by 2030 (Ministry of the Environment, 2023). In Denmark, the polluter-pays principle is applied through direct discharge taxes on total nitrogen (TN) and TP (Konkol et al., 2024) while comparable nutrient-management pressures are also evident in Norway, where high nutrient surpluses and a revised fertilizer policy underscore the need to reduce nutrient losses to water bodies (OECD, 2025; Ministry of Climate and Environment, 2024). In parallel, Nordic greenhouse production often requires substantial supplemental lighting and thermal control due to limited natural irradiance and strong seasonal variability. These requirements further increase the environmental burden of protected cultivation systems, a challenge observed in Finnish greenhouse tomato production, where energy use has been identified as the main contributor to climate impacts (Hernandez Velasco, 2021; Marttila et al., 2021). Under these conditions, microalgae cultivation must be finely tailored to operate within narrow, highly managed indoor envelopes. Nordic greenhouse conditions thus provide a conservative benchmark; performance data obtained under these constrained operating environments can facilitate environmentally sound and resource-efficient greenhouse integrations and support broader deployment of algae-based solutions globally (European Commission, 2022).

This work provides long-term, pilot-scale evidence on integrated microalgae cultivation for agricultural drainwater management under Nordic greenhouse conditions. A continuous phycoremediation system was operated year-round using commercial greenhouse drainwater, evaluating how upstream parameters, from light availability to pH control and nutrient inflow, influence drainwater treatment capacity and EU discharge compliance. The study characterizes the operational trade-offs between biomass productivity and volumetric removal rates, contributing operational practical insights for designing greenhouse-integrated phycoremediation systems that support environmental protection alongside operational feasibility in a circular economy.

2. Materials and methods

2.1. Drainwater characteristics

Drainwater was sourced from a commercial hydroponic cucumber greenhouse - Puutarha Timo Juntti Oy (Kaarina, Finland). All samples were filtered through a 0.2 μm membrane (Minisart® SRP15, Sartorius, Germany) prior to analysis. The physicochemical properties of the drainwater are summarized in Fig. 1, representing the minimum and maximum ranges measured across all collected samples. Preliminary third-party certified laboratory analyses indicated a relatively low organic load in hydroponic drainwater, with COD ranging from 28 to 110 mg L^{-1} and BOD_7 from 3 to 6.3 mg L^{-1} across different sampling time points. A detailed chemical composition of the drainwater can be found elsewhere (Salazar et al., 2021). Corresponding analytical procedures are further detailed in section 2.5.

2.2. Microalgal strain maintenance and scale-up

The *Scenedesmus* sp. NIVA-CHL99 strain was obtained from the Norwegian Culture Collection of Algae (NORCCA) and selected for its robust growth and high nutrient uptake capacity (Salazar et al., 2021). The Scenedesmus genus has been reported to tolerate hydroponic drainwater, ammonium-rich effluents up to approximately 200 mg $N–NH_4^+$ L^{-1} before inhibition, 25–100% municipal wastewater, and organic-rich dairy wastewater containing up to 3500 mg O_2 L^{-1} COD, indicating a broad tolerance to variable inorganic nutrient loads and moderate organic loads (Mercado et al., 2020; Ciardi et al., 2022; Álvarez-Gil et al., 2023; Silambarasan et al., 2023).

Stock cultures were maintained in Z8 medium (Kotai, 1972) at ambient room temperature under continuous low light (10 μmol m^{-2} s^{-1} photosynthetic photon flux density [PPFD]). The culture was scaled up sequentially (50 mL to 500 mL to 5 L), with transfers performed during the exponential growth phase. During this scale up, the strain was cultivated in Z8 under continuous light (70 μmol m^{-2} s^{-1} PPFD), agitated at 100 rpm on an orbital shaker (MIR-S100, Sanyo, Japan), and

B

Characteristics	Unit	Value (min-max)
Conductivity	Sm^{-1}	0.213 - 0.298
pH	-	6.3 -7.4
$N\text{-}NO_3^-$	mgL^{-1}	233 - 422
$P\text{-}PO_4^{3-}$	mgL^{-1}	21 – 49.5
N/P (molar)	-	14 - 37

Fig. 1. Cucumber greenhouse drainwater characterization. **(a)** Visual comparison of the filtered drainwater (left) and the post-harvesting permeate (right). **(b)** Summary table of the drainwater characteristics, including minimum and maximum values.

aerated with 1.5% CO_2-enriched air. The 5 L culture was used as the inoculum for a 65 L closed tubular PBR (details in Valev et al., 2020; modified after Salazar et al., 2023). Prior to use, greenhouse drainwater was filtered through a 0.2 μm membrane filter For each trial, the 65 L PBR was inoculated at an initial OD_{880} of 0.25, corresponding to 0.4 g L^{-1} of biomass. The system was operated in batch mode under a 17 h light:7 h dark photoperiod, provided by LED illumination (6 × NM0004104 VFC, Netled Oy, Finland) at 300 μmol m^{-2} s^{-1}, and supplemented by natural outdoor irradiance. The PBR is housed in a compartment where temperature was maintained at ≥ 20 °C. The culture was constantly aerated with 3% CO_2. Once the density reached OD_{880} > 3.5, measured using a spectrophotometer (section 2.5.3), 50 L of the 65 L culture was harvested to serve as inoculum for the pilot-scale experiments.

2.3. Validation facility setup

The pilot-scale phycoremediation study was performed at the University of Turku's Ruissalo Research Greenhouse (60.433°N, 22.172°E). The validation facility comprises dedicated greenhouse compartments for PBR operations and an on-site analytical laboratory for daily offline analysis and routine monitoring. The complete system, including cultivation, harvesting, and nutrient recycling, is illustrated schematically in Fig. 2.

2.3.1. Greenhouse compartment

The cultivation compartment housed a 1000 L closed tubular PBR system, alongside drainwater and harvesting tanks, membrane filtration units, and a CO_2-injection line (Fig. 2) The greenhouse environment was managed by an automated climate control system that maintained ambient temperatures ≥20 °C. Meteorological data, including outdoor irradiance, day length, outdoor temperature, were continuously monitored and logged at 4-min intervals by an on-site rooftop weather station (ITU Weather Station, Finland). Outdoor irradiance and outdoor temperature values were reported as mean ± SD of daily averages over each operation, consequently the relatively large SD values reflect natural

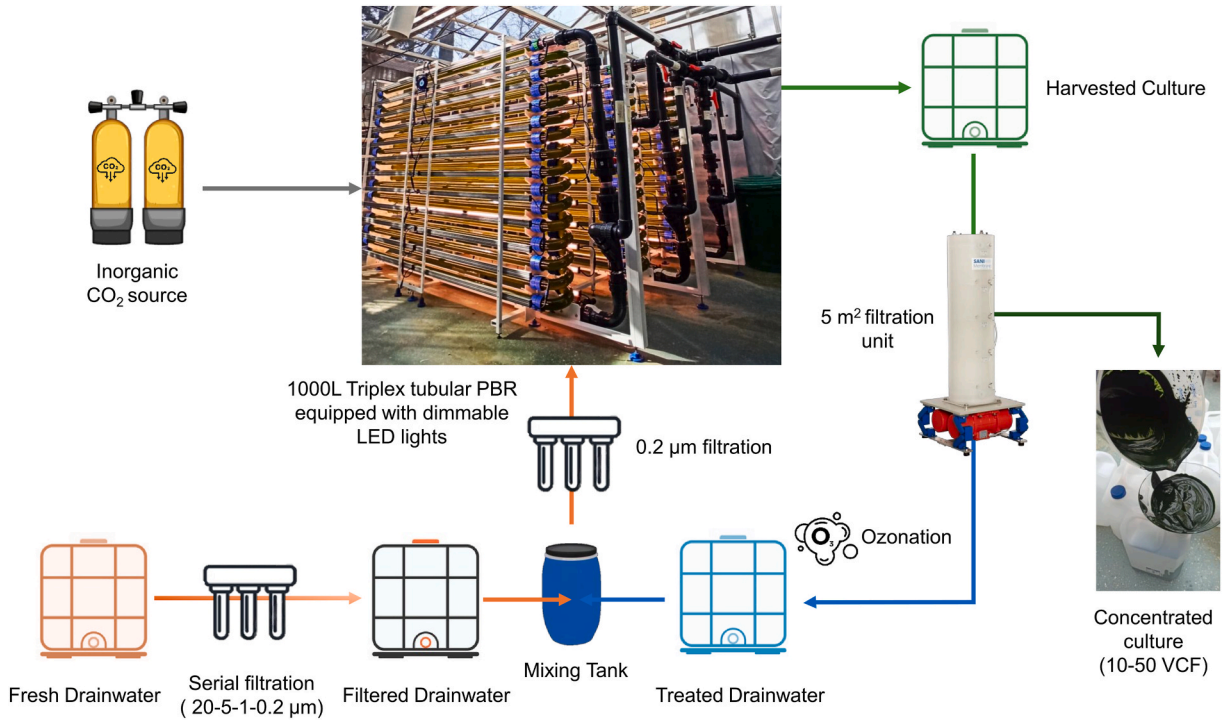

Fig. 2. Schematic overview of the integrated pilot-scale phycoremediation system at the Ruissalo Research Greenhouse, University of Turku. The process flow includes CO_2 supplementation, tubular PBR operation, greenhouse drainwater pretreatment, mixing and dilution, biomass harvesting via membrane filtration, and permeate recycling. VCF: volumetric concentration factor.

day-to-day meteorological variability.

2.3.2. PBR specifications

The core cultivation system consisted of a free-standing 1000 L Triplex Photostage Phyco-Flow™ (Varicon Aqua LTD, UK). This closed tubular PBR comprised three parallel 250 L serpentine photostages, each equipped with isolation valves, and a 300 L main reservoir operating in a closed recirculating loop. This modular configuration allowed for operations at three defined working volumes: 500, 750, and 1000 L. The photostages were Duran®-grade borosilicate glass tubes (Schott, Germany) providing a high surface-area-to-volume ratio essential for optimal light utilization.

Artificial illumination was provided by dimmable LED lights (72 × Flex-Eco S4, Sansol, Austria), positioned bidirectionally at 15 cm from the outer surface of glass tubes. The LEDs offer a spectrum optimized for algal photosynthesis, ensuring stable, continuous phycoremediation performance, particularly during low-light Nordic cold seasons.

Culture circulation was maintained by a low-shear, variable-speed centrifugal pump (Lowara SH 40-160/05, Lenntech, Netherlands), to ensure uniform flow and effective mixing across all photostages. Dissolved oxygen (DO) was managed via air injection ports in each photostage, while biofilm formation was mitigated by an in-line cleaning scrubber (pigging system) that traversed the tubes to preserve light availability.

System operation and monitoring were managed through the VAS AlgaeConnect platform, utilizing in-line probes for optical density (OD_{890}), pH, DO, and temperature. Parameters were recorded every 2 s and logged at 30 s intervals. pH was maintained through threshold-triggered CO_2 dosing under solenoid control. The control unit enables OD-based or time-controlled harvesting, allowing operation in batch, semi-continuous, chemostat, or turbidostat modes.

2.3.3. Nutrient management

Fresh cucumber drainwater was transported regularly from the commercial greenhouse (Puutarha Timo Juntti Oy, Kaarina, Finland) to the validation facility. Upon arrival, it was pre-treated via sequential coarse-to-fine filtration (20 μm→ 5 μm→ 1 μm→ 0.2 μm, BWT Ecosoft SW-PP, Austria). The filtered drainwater was stored in a 1 m^3 bulk supply tank (Fig. 2). The system was designed to automatically dilute fresh drainwater with post-harvesting permeate within a dedicated mixing tank, to facilitate the assessment of various recirculation strategies.

The mixing tank was connected to the PBR via a pressure-sensitive liquid pump (Scala1, Grundfos, Denmark) and an actuated valve, with an in-line 0.2 μm cartridge for sterile delivery. Inflow rates were monitored by an in-line flow meter (Type 335, GF, Switzerland) adjustable between 100 and 600 L h^{-1}. Continuous volume control was maintained with a hydrostatic level sensor in the mixing tank, which regulated automated refilling to meet the PBR's dosing demands. This setup ensured a constant operating volume (1000 L) and supported fully automated media delivery based on the PBR according to operational modes: time-based inflow for chemostat operation or OD-triggered dilution for turbidostat operation. Nutrient concentrations ($N–NO_3$ and $P–PO_4$) content of the fresh drainwater were measured upon the arrival of every new batch, frequently exceeding once a week, while permeate quality was monitored daily.

2.3.4. Harvesting and filtration module

During continuous operation, harvesting was initiated by feeding the drainwater mix into the PBR, displacing an equivalent volume of culture via a harvesting valve positioned at the working-volume level of the main reservoir (Fig. 2). The daily harvest was collected in a dedicated harvesting tank to ensure sufficient minimum volume for membrane filtration. Biomass concentration was performed using a scalable industrial vibrating cross-flow membrane filtration unit (Vibro™ I, SANI Membranes A/S, Denmark), equipped with 2 × DuraPES™ 201 membrane module (polyethersulfone, 0.2 μm pore size, 2.5 m^2 surface area, 3 M Deutschland). The system operated in batch mode, with flow and pressure regulated by centrifugal and pressure pump (SCALA1, Grundfos, Denmark). Operation parameters were maintained at max flow rates of 1 m^3 h^{-1} at 3 Bar (inflow) and 2.2 m^3 h^{-1} at 0.5 Bar (outflow).

The permeate fraction was collected in a separate tank for nutrient recycling and ozonated daily via ozone generator (SP Mural Plus, Cosemar Ozono, Spain) for 10 min at the maximum flow rate to prevent microbial contamination. Harvested culture were concentrated to a final 5–10 L, reaching biomass density of 40–60 g DW L^{-1}. The concentrated biomass was stored at −20 °C for further downstream analysis.

Standard cleaning-in-place (CIP) procedures were performed daily according to the manufacturer's protocols for the harvesting line, collection tanks, and membrane filtration unit. This included pre- and post-filtration rinsing with an alkaline agent (CIP 100™, Steris, US) and sodium hypochloride, followed by a final flush with tap water.

2.4. Experimental design

The experimental framework was designed to evaluate phycoremediation performance across three primary objectives: achieving high biomass productivity, maximizing drainwater-treatment capacity, and ensuring permeate quality for EU-compliant $N–NO_3$ and $P–PO_4$ discharge.

A total of sixteen operations were performed across five trial periods between April 2024 and June 2025. These trials took place in April 2024 (Trial #1), July 2024 (Trial #2), August 2024 (Trial #3), October 2024 (Trial #4), and April 2025 (Trial #5) (Table 1). Operations were run in batch, chemostat, or turbidostat modes. The working volume of all operations was 1000 L, with the exception of Trial #5, which utilized 750 L due to technical constraints.

Operational procedures and modes. All operations followed standardized cultivation parameters. The pH was maintained at 7.5 via automated CO_2 dosing, and constant aeration at a rate of 1.2% (v/v/m). Compartment temperature was maintained at ≥ 20 °C. Artificial light was supplied by LEDs (Section 2.3.2) at 300 μmol m^{-2} s^{-1} under a 17 h:7 h photoperiod (09:00 AM to 02:00 AM), while total light exposure was further influenced by variable natural outdoor irradiance, as detailed in Table 1.

Batch mode (O#1–5). Each trial began with a 7–8 d batch cultivation mode to produce sufficient biomass for continuous operation mode. The batch phase was initiated at an in-line OD_{890} of ≈0.35 and included an initial 24 h adaptation period with LEDs inactive. Once the in-line OD_{890} exceeded 0.4, the culture volume was sequentially increased from 500 L to 1000 L transition to continuous operation was performed after biomass concentration reached 1.79 to 2.32 g L^{-1} across trials (Fig. 3a).

Chemostat mode (O#6–13) was run using time-based influent addition and a single synchronized daily harvesting cycle. Dilution rates were set at 0.2–0.4 d^{-1} with permeate recirculation between 50 and 87.5%, denoting the fraction of permeate returned to the influent stream relative to the total drainwater inflow. These settings corresponded to SRT values of 2.5–5 d and HRT values of 5–20 d (Table 2). SRT–HRT decoupling was achieved via post-harvest membrane filtration process described in Section 2.3.4. Following filtration, the retentate was collected as concentrated biomass and the permeate was partially recirculated to regulate nutrient input while maintaining sufficient residence time for nutrient uptake and discharge compliance.

Turbidostat mode (O#14–16) was implemented after chemostat optimization in Trials #4 and #5 following a brief stabilization period to adjust influent flow rates. In this mode, influent addition and harvesting were controlled by the in-line OD_{890} signal rather than by a preset dilution rate. Three OD_{890} setpoints were tested, namely 0.9 (O#14), 1.2 (O#15), and 1.6 (O#16); selected based on previous operations biomass productivity and seasonal irradiance patterns. All turbidostat trials

Table 1
An overview of 16 operations conducted across five trials including operation modes, meteorological conditions, and drainwater characteristics were represented. Meteorological variables represent daily averages recorded by the on-site station. N–NO_3 and P–PO_4 values reflect the concentration ranges of all fresh drainwater samples used for nutrient load calculations. All operations were conducted at 1000 L working volume unless marked with an astrerisk ([a]), which denotes 750 L.

			Meteorological conditions				Drainwater characteristics	
Operation #	Operation mode	Trial #	Outdoor irradiance (W m^{-2})	Daylight time (h)	$T_{outside}$ (°C)	$T_{compartment}$ (°C)	N–NO_3 (mg L^{-1})	P–PO_4 (mg L^{-1})
O#1	Batch	*T#1 - April '24*	60 ± 23.7	14.0 ± 0.4	3.7 ± 3.0	21.1 ± 1.4	355.9	21.1
O#2		*T#2 - July '24*	98.5 ± 22.6	17.8 ± 0.2	16.8 ± 1.3	24.5 ± 1.1	233.8	21
O#3		*T#3 – August '24*	87 ± 17.9	15.6 ± 0.4	18.5 ± 1.6	23.7 ± 0.5	292.5	31.5
O#4		*T#4 - October '24*	30 ± 14.3	10.1 ± 0.8	8.4 ± 2.7	21.2 ± 0.7	296.5	45
O#5		*T#5 - April '25*	79.5 ± 7.3	13.8 ± 0.3	3.2 ± 3.0	25.9 ± 1.7	257.9	26.7
O#6	Chemostat	*T#1 - April '24*	118.3 ± 8.8	17.4 ± 0.4	18.7 ± 2.6	25.9 ± 1.2	295.1–334.1	18.3–19.5
O#7		*T#1 - April '24*	89.8 ± 24.6	15.5 ± 0.9	6.9 ± 4.9	22.9 ± 1.0	260.2–367.5	8.8–18.2
O#8		*T#3 - August '24*	88.7 ± 15.0	15.0 ± 0.4	17.8 ± 1.1	23.8 ± 0.5	354.6	42.5
[a]*O#9*		*T#5 - April '25*	69.1 ± 27.4	14.3 ± 0.7	6.4 ± 4.9	22.4 ± 1.7	257.9–320.4	26.7–34.4
O#10		*T#2 - July '24*	82.8 ± 33.6	16.8 ± 0.5	19 ± 1.1	25.5 ± 1.1	200.5–301.7	28–42.9
O#11		*T#1 - April '24*	103.7 ± 23.4	17.8 ± 0.7	16.1 ± 3.7	24.3 ± 1.7	266.1–329.4	27.8–34.3
O#12		*T#3 - August '24*	73.6 ± 12.4	14.1 ± 0.4	17.4 ± 1.2	23.8 ± 0.6	281	28
O#13		*T#4 - October '24*	25.8 ± 10.7	9.1 ± 1.2	8.6 ± 2.4	21.4 ± 0.9	336.4	43.3
O#14	Turbidostat	*T#4 - October '24*	14.9 ± 7.4	7.5 ± 1.1	4.8 ± 3.3	21.7 ± 0.6	343.2–421.8	43.3–49.8
[a]*O#15*		*T#5 - April '25*	93.9 ± 14.4	14.3 ± 0.2	6.2 ± 2.8	22.5 ± 0.4	286.6	24.3
[a]*O#16*		*T#5 - April '25*	93.4 ± 32.5	16.9 ± 0.4	10.3 ± 2.9	23.1 ± 0.9	242.9–286	24.3–34.4

[a] Working volume of the operation is 750 L, instead of 1000 L.

operated at a fixed 75% permeate recirculation, maintaining an HRT approximately four times the SRT (HRT = 4 × SRT). To filter sensor noise, harvesting was triggered or stopped only when the in-line OD_{890} remained above or below the selected setpoint for 6 s corresponds to three consecutive readings.

2.5. Analytical procedures

2.5.1. In-line monitoring and meteorological data

In-line OD_{890}, pH, temperature, and DO were recorded at 30 s intervals through PBR control software (VariConnect, Varicon Aqua, UK). Meteorological variables (outdoor irradiance, outdoor temperature and compartment temperature) were logged at 4-min intervals via the on-site weather station server (ITU CAG Visual MS10, Finland) (Table 1).

2.5.2. Sampling

Daily samples (≥25 mL) were collected from four points: the culture in the PBR, harvested culture, filtration retentate (concentrated biomass), and permeate tank. During chemostat operations, additional samples were taken immediately before and after the daily harvest. Fresh drainwater was sampled for N–NO_3 and P–PO_4 analysis upon the arrival of each new batch and monitored periodically during storage. All samples were analyzed immediately or stored at 4 °C for analysis within the same day.

2.5.3. Offline measurements

Biomass concentration was determined gravimetrically as DW. Culture samples were filtered through pre-dried, pre-weighed glass microfiber filters (Whatman GF/F, 0.7 μm), dried at 95 °C to a constant weight, and reweighed after cooling in a desiccator. Offline OD measurements at 680, 750, and 880 nm were recorded using a UV-Vis spectrophotometer (GENESYS 2, Thermo Spectronic, USA) to establish correlations with DW and inline OD_{890} readings (Supplementary Fig. S1).

The supernatant from DW determination was used for nutrient analysis. N–NO_3 concentrations were quantified according to the APHA 4500-NO_3-B (APHA, 1992), and P–PO_4 was determined using orthophosphate test kit (Spectroquant 114,842, Merck, Germany). Calibration curves were prepared from $NaNO_3$ (>99%, Merck) and K_2HPO_4 (99%, VWR) standards. The pH of fresh drainwater was measured using an on-site pH probe. Conductivity was determined with a handheld conductivity meter (LAQUAtwin EC-33, Horiba, Japan). All DW, OD, and nutrient measurements were performed in triplicate. A standard light microscope (Researcher Trino, Bresser, Germany) was used for routine assessment of culture quality.

2.5.4. Calculations

Daily biomass productivity (P_x, g L^{-1} d^{-1}) was calculated from offline dry weight (DW) measurements as:

$$P_x = \frac{DW_{\text{final}} - DW_{\text{initial}}}{t_{\text{final}} - t_{\text{initial}}} \quad (1)$$

where $DW_{initial}$ and DW_{final} represent the biomass DW concentrations (g DW L^{-1}) measured at the beginning and end of the calculation interval, respectively; and $t_{final} - t_{initial}$ denotes the elapsed time (d). For daily productivity calculations, consecutive sampling points were utilized ($\Delta t = 1$ d). The application of this definition varied according to the operation modes. In batch mode, daily P_x values were calculated during the exponential-growth phase and subsequently averaged. In chemostat mode, daily biomass productivity (P_x) was calculated using Eq. (1), where DW_{final} was measured immediately prior to harvesting and as $DW_{initial}$ immediately following harvesting. The resulting biomass difference was defined as the harvested biomass and expressed as daily biomass productivity.

In turbidostat mode, where culture DW remained stable, daily P_x (g L^{-1} d^{-1}) was calculated from the harvested biomass as:

$$P_{x,\text{turbidostat}} = \frac{DW_{\text{harvest}} \times V_{\text{harvest}}}{V_{\text{working}}} \quad (2)$$

where DW_{harvest} is the DW of the harvested culture (g L^{-1}), V_{harvest} is the daily harvested volume (L), and V_{working} is the working volume of the PBR (L).

Daily nutrient-uptake rates (r_x, with x representing N–NO_3 or P–PO_4) were calculated using the general definition:

$$r_x = \frac{C_{x,i} - C_{x,i+1}}{\Delta t} \quad (3)$$

where $C_{x,i}$ and $C_{x,i+1}$ are nutrient concentrations (mg N–NO_3 L^{-1} or mg P–PO_4 L^{-1}) on consecutive days, and $\Delta t = 1d$.

Across operation modes, the uptake calculation followed different procedures. In batch mode, uptake values from the exponential growth phase were averaged. In chemostat mode, the concentration difference between the after harvesting sample of Day *i* and the before harvesting

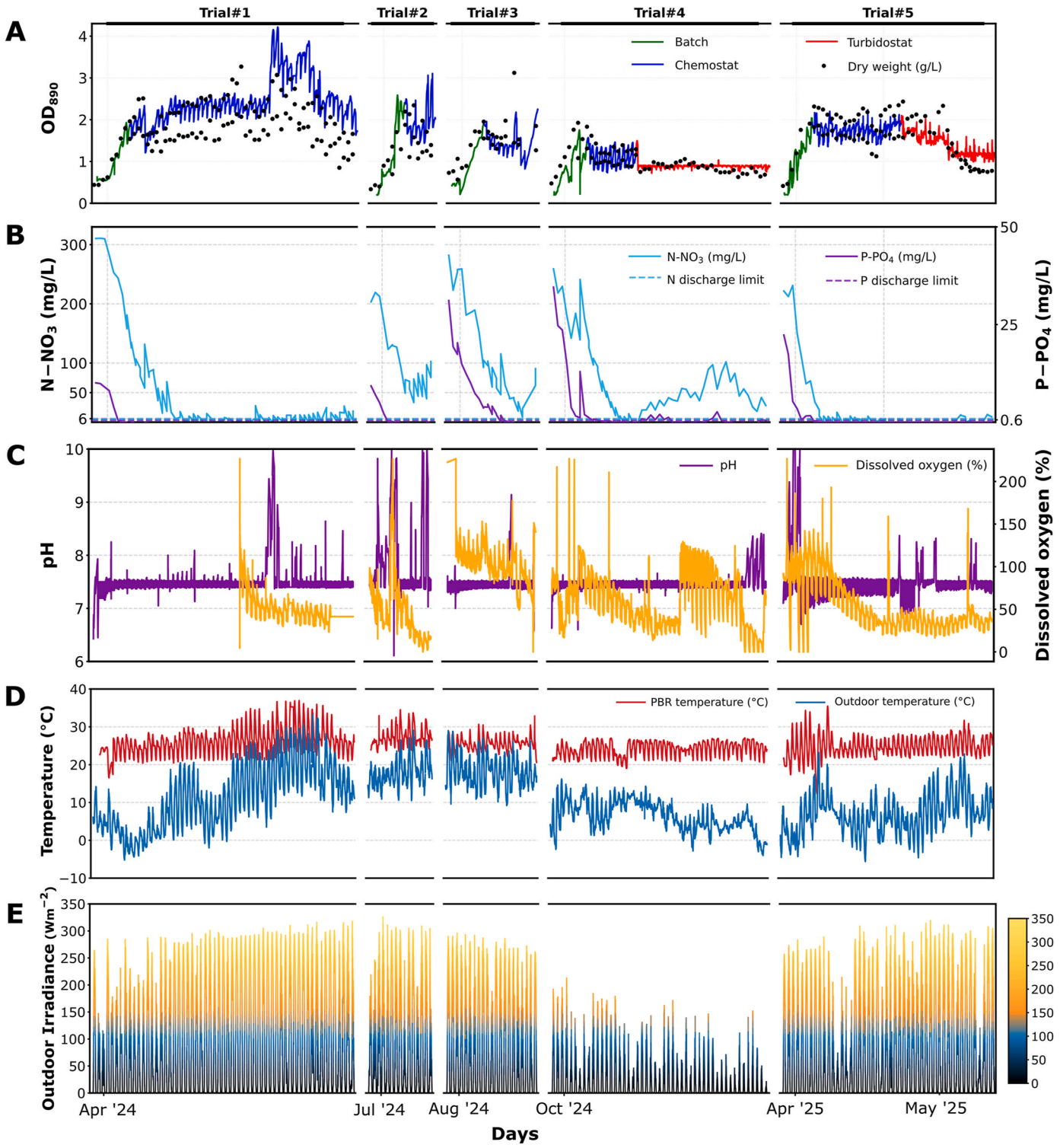

Fig. 3. Operational and performance data for pilot-scale phycoremediation in a pilot scale PBR. Five continuous trials (T1 to T5) were performed over an extended period from April 2024 and June 2025 in a controlled greenhouse. Vertical dashed lines indicate reactor inoculations marking the start of each trial. Trial durations: T1: 12.04.2024-17.06.2024 (66 d), T2: 03.07.2024-22.07.2024 (19 d), T3: 06.08.2024-27.08.2024 (21 d), T4: 03.10.2024-28.11.2024 (56 d), T5: 08.04.2025-26.05.2025 (48 d) **(a)** Biomass concentration profiles for different cultivation modes: Batch (green line), chemostat (blue line), and turbidostat (red line). Data include inline OD_{890} and daily dry weight (black dots) from offline measurements. **(b)** $N–NO_3$ and $P–PO_4$ uptake performances of the culture. Horizontal dashed lines represent EU discharge limits (6 mg L^{-1} for $N–NO_3$ and 0.5 mg L^{-1} for $P–PO_4$. **(c)** Culture physicochemical parameters. Inline monitoring of the culture pH (purple line) and dissolved oxygen (DO, % saturation; orange line). **(d)** Temperature profiles. Comparison of outdoor ambient temperature (blue line) and PBR culture temperature (red line) **(e)** Outdoor solar irradiance profiles. Outdoor solar irradiance (W m^{-2}) during the cultivation period, displayed by a color gradient (blue to yellow) representing seasonal fluctuations.

Table 2
Overview of sixteen operational configurations evaluated in the pilot-scale phycoremediation system.

Operation #	Operation Mode	Trial #	Operation time (d)	SRT (d)	HRT_{fresh} (d)	OD set point	Nutrient-free permeate
O#1	Batch	*T#1 - April '24*	7	-	-	-	
O#2		*T#2 - July '24*	8				
O#3		*T#3 - August '24*	8				
O#4		*T#4 - October '24*	8				
O#5		*T#5 - April '25*	7				
O#6	Chemostat	*T#1 - April '24*	16	5	10	-	✔
O#7		*T#1 - April '24*	26		20		✔
O#8		*T#3 - August '24*	7				✖
[a] ***O#9***		*T#5 - April '25*	20				✔
O#10		*T#2 - July '24*	7	2.5	5		✖
O#11		*T#1 - April '24*	10		10		✔
O#12		*T#3 - August '24*	6		20		✔
O#13		*T#4 - October '24*	11				✔
O#14	Turbidostat	*T#4 - October '24*	30	2.94[b]	11.8[b]	0.9	✖
[a]***O#15***		*T#5 - April '25*	11	2.22[b]	8.9[b]	1.2	✔
[a]***O#16***		*T#5 - April '25*	10	3.57[b]	14.3[b]	1.6	✔

[a] Working volume of the operation is 750 L, instead of 1000 L.
[b] Calculated SRT and HRT values.

sample of Day $i+1$ represented the uptake for Day i. In turbidostat mode, culture concentrations alone were not informative; therefore, uptake (mg N–NO_3 L^{-1} d^{-1}) was calculated as:

$$r_{x,\text{turbidostat}} = \frac{C_{x,i} + C_{\text{inflow}} - C_{x,i+1}}{\Delta t} \quad (4)$$

with the theoretical nutrient input C_{inflow} (mg N–NO_3) defined as:

$$C_{\text{inflow}} = \frac{V_{\text{fdw}}\, C_{\text{fdw}} + V_{\text{permeate}}\, C_{\text{permeate}}}{V_{\text{total inflow}}} \quad (5)$$

where V_{fdw} and V_{permeate} denote daily volumes of fresh drainwater and permeate added, and C_{fdw} and C_{permeate} (mg N–NO_3) their corresponding nutrient concentrations.

SRT (d) was calculated as:

$$SRT = \frac{1}{D} \quad (6)$$

where D (dilution rate, d^{-1}) was predetermined in chemostat mode, while in turbidostat mode the actual dilution rate (d^{-1}) was calculated as:

$$D_{\text{turbidostat}} = \frac{V_{\text{harvest}}}{V_{\text{working}}} \quad (7)$$

where V_{harvest} is the daily volume removed during automatic harvesting (L) and V_{working} is the reactor working volume (L). HRT (d) was calculated using the relationship:

$$HRT = \frac{1}{D(1-r)} \quad (8)$$

where r is the recirculation coefficient (e.g., 75% recirculation → $r = 0.75$).

2.6. Statistical analysis

Pairwise Pearson correlation analysis evaluated linear associations among biomass productivity, nitrate uptake, hydraulic parameters, and meteorological drivers. Correlation strength ranged from −1 (negative association) to +1 (positive association). Statistical significance was set at $p < 0.05$ unless stated otherwise. Analyses were conducted in Python using pandas, SciPy, and Matplotlib libraries. Operational data from batch, chemostat, and turbidostat phases were evaluated both collectively and mode-specifically to interpret performance trends across varying hydraulic and environmental conditions.

3. Results and discussions

3.1. Continuous year-round phycoremediation sustains hydroponic drainwater treatment and algal biomass production

To evaluate the long-term feasibility of agricultural drain water remediation and subsequent algal biomass production in a Nordic climate, we selected *Scenedesmus* sp. NIVA-CHL 99, a strain previously identified as promising (Salazar et al., 2021). Validation experiments were conducted in a 1000 L tubular PBR located within a controlled research greenhouse at the University of Turku's AlgaTech facility. For all operations, artificial LED lights provided 300 μmol m^{-2} s^{-1} light intensity in a diurnal 17 h on −7 h off cycle, where the lights turned on at 9AM and turned off at 2AM.

A total of five distinct, continuous cultivation trials were performed spanning from April 2024 to June 2025, with each trial representing a period under seasonal and environmental conditions. Within these trials, sixteen different operations were tested for specific system parameters. These operations employed three PBR operation modes: five batch, eight chemostat, and three turbidostat (Table 1). The trials were specifically scheduled to present both colder and warm seasonal conditions, allowing for assessment of the system's performance, repeatability and stability across different seasons. Fig. 3 shows the operational and performance data gathered across the five trials, demonstrating the system's response to varying environmental conditions. These operational changes specifically tested performance against the inherent process variabilities: the significant fluctuations in the natural light and temperature typical of the Nordic climate (Fig. 3d and e) and the variable nutrient concentrations of the agricultural drain water (Fig. 3b), which fluctuate based on the crop stage, fertigation schedules and crop harvesting seasons. Although this study focused on N–NO_3 and P–PO_4 as the dominant fertilizer-derived compounds, the low organic load of the influent (COD 28–110 mg L^{-1}, BOD_7 3–6.3 mg L^{-1}) indicated that, under commercial greenhouse conditions, the drainwater is predominantly inorganic. Trial durations ranged from three to nine weeks.

Seasonal variations and systems stability. Daylight varied drastically, ranging from 6.4 h (November 2024) to 18.5 h (June 2024). Irradiance showed a clear seasonal pattern, with the highest instantaneous outdoor irradiance reaching 333 W m^{-2}. The daily average outdoor irradiance peaked during May–June 2024 (118.3 ± 8.8 W m^{-2}), dropped to its lowest during October–November 2024 (14.9 ± 7.4 W m^{-2}) (Fig. 3e). While outdoor temperatures fluctuated widely (e.g., +33.2 °C on May 2024; −5.6 °C on April 2025), the greenhouse compartment maintained a daily average temperature between 21.1 °C

and 25.9 °C. The PBR culture temperature ranged 16.8 °C (April 2024) to a maximum of 36.9 °C (May 2024). This thermal profile demonstrates both the robustness of *Scenedesmus* sp. NIVA-CHL99 strain and the stable performance of the system across this operational range (Fig. 3d).

The pH was tightly controlled and remained stable at 7.5 ± 0.1 for 91 % of the operational period (Fig. 3c). DO concentration of the culture managed via constant aeration (1.2% v/v/min) showed the expected diurnal fluctuations (Fig. 3c) linked to solar irradiance and photosynthetic activity (Díez-Montero et al., 2020; Masojídek et al., 2024).

PBR operation modes. In this long-term study, three PBR operation modes - batch, chemostat, and turbidostat - were employed sequentially across sixteen operational configurations. The primary operational challenge, especially for the continuous modes, was managing the high nutrient load of the drain water while ensuring the treated effluent (permeate) met the EU discharge limits. Initial N–NO_3 and P–PO_4 concentrations across the five trials ranged between 204.7 and 310.4 mg L^{-1} and 9.3–34.5 mg L^{-1}, respectively (Fig. 3b). Each trial began with an initial 7–8 days batch cultivation allowing the culture to reach the required biomass concentration (1.79–2.32 g L^{-1}) before transitioning to continuous operation (Fig. 3a).

Following the initial batch phase, the PBR system was transitioned to chemostat operation, synchronized with a single daily biomass harvest to maximize nutrient removal efficiency. A key operational challenge was the trade-off between achieving high biomass productivity, favoured by short solid retention times (SRT), and ensuring complete bioremediation of N-rich drainwater, which requires long hydraulic retention times (HRT). To resolve this, a post-harvest tangential-flow filtration coupled with permeate recycling was implemented, effectively decoupling HRT from SRT. Following filtration, the retentate (concentrated biomass) was collected, while the permeate (treated drainwater) was partially recirculated (50–87.5%). This controlled recycling strategy provided adequate yet non-excessive nutrient supply entering PBR, ensuring sustained biomass productivity while maintaining sufficient residence time for complete nutrient uptake and discharge compliance.

The experimental design systematically studied the impact of dilution rate and permeate recirculation on phycoremediation by testing various HRTs (5–20 d) to optimize performance for regulation-compliant permeate discharge. In chemostat mode, compliant discharge was achieved at dilution rates up to 0.4 d^{-1} when recirculation was maintained at > 75%. Conversely, higher dilution rates or lower recirculation led to excessive daily nutrient loading, nutrient accumulation in the permeate and loss of compliance (e.g., O#10). After optimizing chemostat parameters, the system transitioned to turbidostat mode in Trials #4 and #5, following a brief stabilization period to adjust influent flow rates. In these trials, the recirculation ratio was fixed at 75%, establishing a controlled decoupling where HRT was maintained at approximately four times the SRT (HRT = 4 × SRT).

Biomass productivity. Throughout all trials, biomass concentration was monitored via inline optical density probe at 890 nm (OD_{890}) for real-time control, validated through offline DW measurements, confirming stable production under both continuous modes (Fig. 3a).

Continuous cultivation of *Scenedesmus* sp. NIVA-CHL 99 yielded daily average biomass productivities ranging from 0.30 to 0.68 g L^{-1} d^{-1}, outperforming the exponential stage of batch cultivation (0.22–0.32 g L^{-1} d^{-1}). In turbidostat mode, three fixed OD_{890} setpoints (O#14: 0.9, O#15: 1.2, O#16: 1.6) yielded average biomass productivities of 0.30–0.55 g L^{-1} d^{-1} based on harvested volume. While turbidostat productivity was comparable to chemostat performance under similar meteorological conditions, it demonstrated superior phycoremediative potential (see section 3.2).

During the first turbidostat operation (T#4, O#14), the OD_{890} threshold was set at 0.9, considering the relatively low light availability and biomass productivity previously observed under batch cultivation. However, this trial was affected by unusually high influent concentrations of cucumber greenhouse drainwater (343–422 mg N–NO_3 L^{-1}, 43.3–45.0 mg P–PO_4 L^{-1}), which impacted the nutrient intake–uptake balance and hindered complete daily nutrient removal. This was mitigated in subsequent operations (O#15, O#16), by dynamically adjusting OD thresholds as nutrient levels returned to typical ranges.

The EU discharge compliance. The system was strategically operated to ensure robust nutrient removal, yielding treated drainwater (permeate) that met EU discharge compliance immediately after culture harvesting. Despite continuous drainwater addition, the daily nutrient uptake rate and effective harvesting strategy ensured that concentrations of both N and P consistently remained below regulatory discharge limits throughout the operations (Fig. 3b). Notably, the system often succeeded in driving these nutrient concentrations to near-zero levels in the permeate, significantly exceeding regulatory requirements. While similar continuous cultivation modes (chemostat and turbidostat) have been previously studied for wastewater treatment, those studies typically did not prioritize achieving post-harvest, regulation-compliant discharge quality (Aparicio et al., 2024; Morillas-España et al., 2024). To the best of our knowledge, the present work represents the first long-term phycoremediation study conducted in turbidostat mode using real greenhouse drainwater, characterized by high and variable nutrient loads, that simultaneously maximized drainwater treatment capacity and produced permeate meeting regulatory discharge standards at the 1000 L pilot-scale.

3.2. Nutrient removal efficiency and drainwater treatment performance

The drainwater treatment performance of the pilot-scale phycoremediation system was evaluated based on daily N–NO_3 and P–PO_4 removal rates across sixteen distinct operations (O#1–16). While N–NO_3 concentrations in the culture medium exhibited dynamic variations, P–PO_4 levels were only detectable during the initial batch phases. Throughout most of the continuous operations, phosphate remained below the detection limit of the analytical kit (2.5 μg P–PO_4 L^{-1}) (Fig. 3b).

Complete P–PO_4 removal was generally achieved within the first 4–6 days of batch cultivation, with uptake rates of 3.43–3.49 mg L^{-1} d^{-1} (Fig. 3b). Such rapid depletion is characteristic of luxury P uptake, where high-affinity transporters and intracellular polyphosphate storage allow cells to accumulate phosphate beyond immediate metabolic requirements (Solovchenko et al., 2019). During the short periods when P–PO_4 was measurable, removal rates showed only modest sensitivity to irradiance ($r = -0.29$), temperature ($r = -0.30$), and N–NO_3 uptake ($r = -0.43$). This negative correlation between N and P uptake suggests a temporary kinetic decoupling of nutrient assimilation due to the nitrate-rich medium as utilized here. Instead, initial P–PO_4 availability ($r = 0.51$) acted as the primary driver of depletion dynamics. This phosphate depletion in the effluent resulted from an increasing N:P molar ratio in the culture medium during continuous operations. This shift was driven by the selective retention of higher residual N–NO_3 concentrations via permeate recirculation, aimed at achieving discharge compliance. Given the consistent near-complete P–PO_4 removal under continuous operation, the system's drainwater treatment performance was evaluated primarily through daily N–NO_3 removal. This focus is further supported by the low organic load of the influent drainwater, indicating that the removal of dissolved inorganic nutrients—rather than the treatment of organic carbon—constituted the main remediation challenge under the present operating conditions.

Batch operations (O#1–5) demonstrated robust N–NO_3 removal, with daily uptake rates ranging from 19.7 to 33.1 mg L^{-1} d^{-1} and removal efficiencies of 40.4–84.4% within 7–8 days (Fig. 3b). During the exponential phase, N–NO_3 uptake exhibited a positive correlation with daily irradiance ($r = 0.72$), implying that light availability was a key driver of nitrate removal. This aligns with previous findings that phototrophic nutrient uptake is closely coupled to irradiance (Gonçalves et al., 2014; Rani and Maróti, 2023). Indeed, batch operations conducted in spring (O#1, O#5) yielded the most efficient N–NO_3 removal, whereas autumn batch (O#4) showed reduced performance due to

lower irradiance (30 ± 14.3 W m^{-2}) and a lower N/P ratio (14.1). The ratio between average nitrogen uptake and biomass productivity ($r_{n\ N–NO3}/P_x$ = 7.5–15%) demonstrated a proportional relationship between nutrient consumption and biomass growth, implying efficient nitrogen utilization under non-limiting nutrient conditions. Chemostat operations (O#6–13) were employed to regulate nutrient inflow and maintain compliant discharge by adjusting dilution rate (0.2–0.4 d^{-1}) and permeate recirculation ratios (50–87.5%). These operations served as operational benchmarks for subsequent turbidostat trials by identifying hydraulic and nutrient parameters necessary to balance nutrient supply with cellular uptake while maintaining discharge compliance.

Daily N–NO_3 uptake in chemostat operations (O#6–13) ranged from 7.1 to 28.8 mg L^{-1} d^{-1} (Fig. 4a), primarily influenced by nutrient loading rates, hydraulic retention time, and seasonal irradiance (Tables 1 and 2). The first chemostat (O#7) operated for 26 days with the longest HRT_{fresh} (20 d) and moderate recirculation (75%), yielding an average N–NO_3 uptake of 17.9 mg L^{-1} d^{-1}. During O#7, permeate nitrate concentrations remained below 6 mg L^{-1} (EU discharge limits) for 38 consecutive days; a similar compliance level was later reproduced under optimized turbidostat operations (Fig. 3b).

When the HRT was halved to 10 d in O#6 following the O#7 (5 d SRT, 75% recirculation), daily N–NO_3 uptake dropped significantly to 9.1 mg L^{-1} d^{-1}, the second lowest of all sixteen operations, despite a 100 L d^{-1} fresh drainwater inflow (Fig. 4c). Increasing harvesting and inflow volumes in O#11 (10 d HRT, 2.5 d SRT) elevated N–NO_3 uptake to 14.3 mg L^{-1} d^{-1}, highlighting the sensitivity of nutrient removal performance to hydraulic conditions. In Trials #2–3, shorter HRTs (5–10 d) and higher nutrient loadings enhanced nitrate uptake. While O#8 reached the highest chemostat removal rate (28.8 mg L^{-1} d^{-1}), O#10 achieved a comparable uptake rate (25.0 mg N–NO_3 L^{-1} d^{-1})

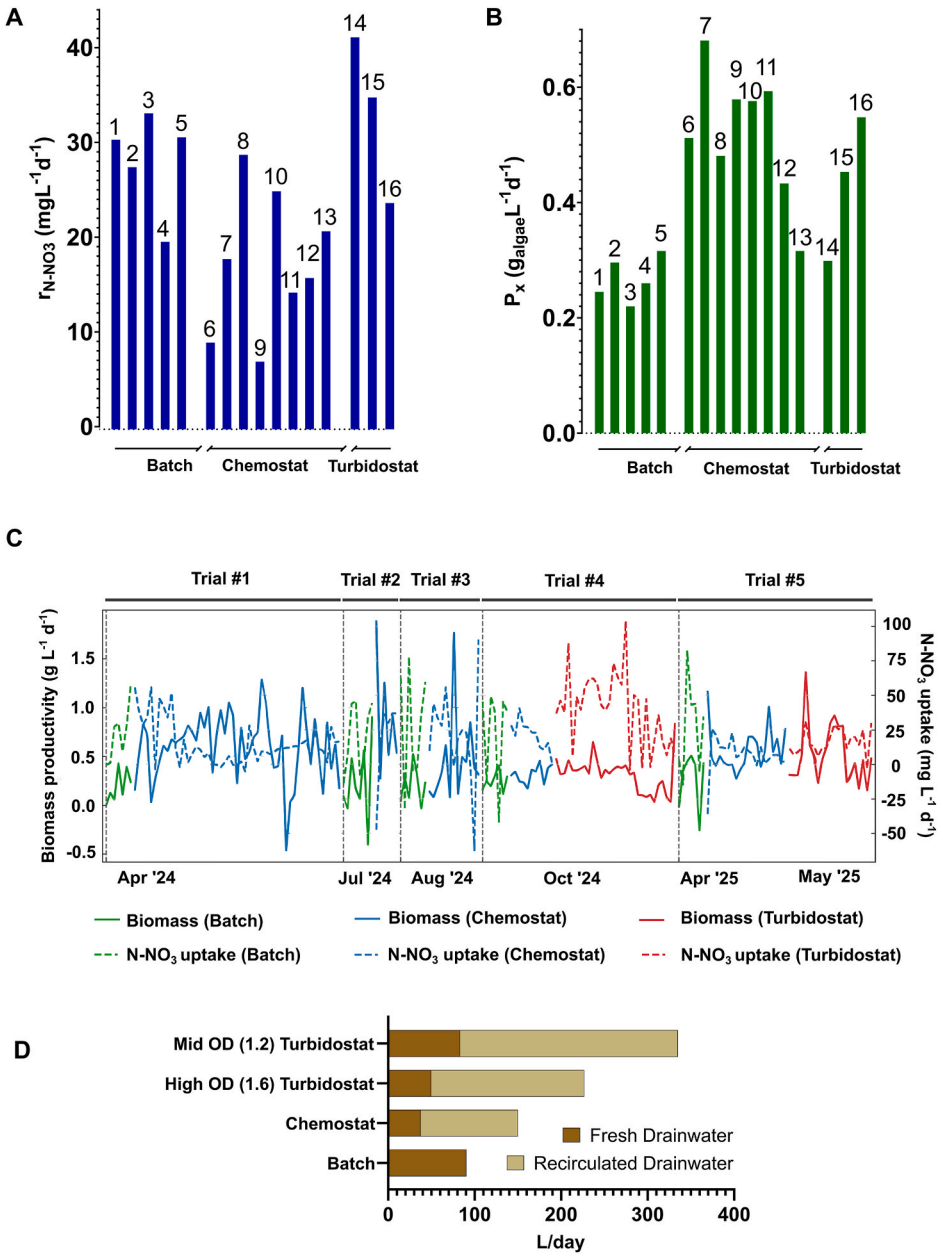

Fig. 4. Biomass productivity and nitrate uptake dynamics across operation modes. Daily average of **(a)** N–NO_3 uptake and **(b)** volumetric biomass productivity for all operation modes. Numbers on the bar graph represent operation numbers. **(c)** N–NO_3 uptake and volumetric biomass productivity of every operation day across five trials. Daily biomass productivity (solid line) and N–NO_3 uptake (dashed line) for year-round phycoremediation. **(d)** Daily volumes of fresh drainwater and recirculated permeate treated in Trial #5 across batch, chemostat, and turbidostat at OD_{890} = 1.2 and 1.6.

despite receiving the highest nutrient input (65 mg N–NO_3 L^{-1} d^{-1} with 200 L d^{-1} fresh drainwater inflow). However, this operational regime resulted in effluent nitrate and phosphate concentrations to exceed discharge limits, reaching up to 94.8 mg L^{-1} N–NO_3, and 2.7 mg L^{-1} P–PO_4 in the permeate (Fig. 3b). In contrast, the hydraulic variables in chemostat O#9 in Trial #5 (20 d HRT, 5 d SRT) resulted in the lowest uptake of 7.1 mg L^{-1} d^{-1}. Overall, chemostat operations ensured stable and controlled nutrient removal under balanced dilution and recirculation regimes. However, their long-term treatment robustness was inherently limited by the trade-off between maximizing nutrient processing rates and maintaining discharge compliance.

P–PO_4 inflow played a key role in sustaining high N–NO_3 uptake during continuous operations. In O#8 and O#13, higher P–PO_4 concentrations in the fresh drainwater (42.5–43.3 mg L^{-1}) increased the overall P availability in the medium throughout both chemostat runs. This elevated P supply supported higher N–NO_3 uptake capacities, reaching 28.8 mg L^{-1} d^{-1} in O#8 and 20.8 mg L^{-1} d^{-1} in O#13.

Although biomass productivity was strongly influenced by outdoor irradiance (0.45 g L^{-1} d^{-1} under 88.7 ± 15.0 W m^{-2} in O#8 versus 0.32 g L^{-1} d^{-1} under 25.8 ± 10.7 W m^{-2} in O#13), N–NO_3 uptake did not follow the same light-dependent trend. Under these specific nutrient-limited steady-state conditions, P inflow and the resulting molar N:P ratio appeared to be more influential drivers of nitrogen removal performance than irradiance. This indicated that the system was primarily P-limited, which therefore decoupled N-uptake kinetics from the diurnal light regime.

Turbidostat operations (O#14–16) demonstrated the highest drainwater treatment performance, sustaining high N and P removal without substantial losses in biomass productivity. The first pilot-scale turbidostat was initiated on 22 October 2024 (O#14; OD_{890} setpoint = 0.9, 75% recirculation), lasted 30 days, and produced an average daily harvest of 341.6 L d^{-1} (45–670 L d^{-1}, median 380 d^{-1}), with volumes driven by day-to-day differences in biomass growth under fluctuating outdoor irradiance. The light periods in the first three weeks routinely triggered harvesting around 400–600 L d^{-1}, whereas the final nine days coincided with the lowest irradiance (5.9–10.4 W m^{-2}) and shortest daylight hours (7.1–7.9 h) of the operation, reducing harvest volumes to 45–120 L d^{-1}. Despite this, O#14 achieved the highest daily N–NO_3 uptake of all operations (41.1 mg L^{-1} d^{-1}) (Fig. 4a). However, the extreme influent drainwater concentrations (343–422 mg L^{-1} N–NO_3; 43–45 mg L^{-1} P–PO_4) disrupted the balance between nutrient inflow and cellular uptake. This imbalance temporarily led to compliance failure and produced the highest permeate nutrient concentrations recorded during the trials, up to 102 mg N–NO_3 L^{-1} and 2.67 mg P–PO_4 L^{-1}, significantly exceeding the permitted regulatory discharge limits. These findings highlight the inherent trade-off between maximizing nutrient removal performance and maintaining compliant effluent quality under high nutrient loading conditions.

Subsequent turbidostat operations in Trial #5 were designed to optimize nutrient input-cellular uptake dynamics based on insights from previous chemostat and turbidostat operations. The high-OD turbidostat (O#16; OD_{890} setpoint = 1.6) operated for 10 days, during which 2267 L of drainwater were utilized (496 L fresh; 1771 L recirculated), resulting in 0.302 d^{-1} dilution rate. Within this regime, 49.6 Ld^{-1} of fresh drainwater, 6.6% of the 750 L working volume, were utilized while still maintaining EU-compliant permeate quality and an average N–NO_3 uptake of 17.8 mg L^{-1} d^{-1}.

Based on the operational limits observed at OD_{890} = 0.9 (high N uptake, compliance failure) and OD_{890} setpoint of 1.6 (stable compliance, low treatment capacity), an intermediate OD_{890} setpoint of 1.2 was selected for O#15 (mid-OD turbidostat). N–NO_3 and P–PO_4 concentrations of the drainwater utilized were the same in O#15 and O#16. O#15 operated for 11 days and resulted in a dilution rate of 0.446 d^{-1}, during which it treated a total of 3684 L of drainwater (916 L fresh; 2769 L recirculated). Under these operational conditions, O#15 increased total and fresh drainwater treatment capacities by 47.7% and 67.7%, respectively, compared with O#16 (Fig. 4d). Fresh drainwater treated equaled 11.1% of the PBR volume per day, and N–NO_3 uptake rose to 26.1 mg L^{-1} d^{-1} (Fig. 4a), representing 46.6% more N–NO_3 removal compared to O#16. Although daily biomass productivity was 27.8% lower than in O#16, O#15 delivered the most favorable balance between nutrient removal performance and regulatory discharge compliance in this study. This underscores the potential of controlled turbidostat operation for large-scale phycoremediation in Nordic greenhouse environments.

3.3. Microalgae biomass productivity by operation modes

During the five trials performed between April 2024 and June 2025, biomass productivity was monitored daily based on dry weight, inline OD_{890} readings, and offline OD_{880} measurements. The biomass concentration in the PBR ranged from 0.3 to 3.5 g L^{-1} (Fig. 3a). Before the turbidostat experiments were initiated, the response range of the in-line OD_{890} probe was assessed against offline OD_{880} and DW measurements (Supplementary Fig. S1). This assessment indicated that OD_{890} values below 0.9 were noisy and poorly correlated with biomass, whereas values above 1.2 indicated the onset of signal saturation. Accordingly, 0.9 and 1.2 were selected as turbidostat setpoints within the probe's linear response range. A higher setpoint of 1.6 was also included to examine turbidostat operation near the upper measurable limit, where reduced responsiveness was expected. This allowed to evaluate the behavior and stability of turbidostat control under conditions approaching the probe's saturation boundary. Overall, DW data were primarily used for biomass productivity calculations, while in-line OD_{890} signal served for trend monitoring throughout the study.

Batch operations (O#1–5) ran for 7–8 days and were initiated with a one-day inoculation period under natural daylight only (artificial lights off). In batch mode, average biomass productivity ranged between 0.22 and 0.32 g L^{-1} d^{-1}, representing the lowest productivity among the three operation modes (Supplementary Fig. S2). The highest productivity in batch mode (0.32 g L^{-1} d^{-1}) was achieved in O#5, which was operated under moderate outdoor irradiance (79.5 ± 7.3 W m^{-2}) and favorable temperature (25.9 ± 1.7 °C). O#2 and O#4 showed intermediate productivities (0.30 and 0.26 g L^{-1} d^{-1}) under higher irradiance (98.5 ± 22.6 W m^{-2} and 30 ± 14.3 W m^{-2}, respectively) and comparable culture temperatures (Fig. 3d and e). The lowest productivities were recorded in O#1 and O#3 (0.25 and 0.22 g L^{-1} d^{-1}, respectively), both associated with suboptimal irradiance conditions resulting from seasonal variation in the light regime.

Chemostat operations (O#6–13) achieved the highest biomass productivity among all operation modes (0.52 ± 0.11 g L^{-1} d^{-1}). In Trial #1, O#7 operated with the highest HRT and SRT, minimized daily nutrient inflow, and ran for 26 days. Under these conditions, the maximum biomass productivity observed in this study was 0.68 g L^{-1} d^{-1} with culture DW ranging from 1.69 to 3.53 g L^{-1} (Fig. 3a). N–NO_3 was available at the start of O#7, indicating the absence of nutrient stress, while outdoor irradiance and photoperiod were favorable (65.2–126.3 W m^{-2}; 14.6–18.2 h daylight). This maximum productivity was achieved under favorable conditions of high light and temperature, minimal nutrient input, low residual nutrient concentrations, and no detectable biotic stress supported by microscopy imaging. A total of 17.6 kg of biomass was harvested during the 26-day operation.

In O#6, halving the HRT compared to O#7 while maintaining SRT constant, led to a higher nutrient inflow and a biomass productivity of 0.51 g L^{-1} d^{-1} (Fig. 4b). The final chemostat operation in Trial #1 (O#11) tested the shortest SRT (2.5 d) and the highest dilution rate (0.4 d^{-1}). Doubling the dilution rate in O#11 halved the culture DW as expected (from 3.0 to 1.5 g L^{-1}) (Fig. 3a), which in turn slightly improved the biomass productivity to 0.59 g L^{-1} d^{-1} (Fig. 4b), likely due to enhanced light penetration (Barbera et al., 2020). Trial #1 was terminated after heterogeneity was observed due to accumulated sedimentation in PBR (Fig. 6a).

Three chemostat operations were conducted in Trials #2 and #3 (O#8, O#10, O#12). These operations were shorter than others due to contamination that formed within three weeks after inoculation under summer greenhouse conditions (Fig. 6b). O#10 tested the lowest SRT and HRT (2.5 and 5 d, respectively) under high and variable irradiance (82.8 ± 33.6 W m^{-2}). The combination of the highest N–NO_3 inflow (65 mg L^{-1} d^{-1} N–NO_3), with high dilution rate, affected light penetration but still yielded a biomass productivity of 0.58 g L^{-1} d^{-1}. O#8, replicating O#7 conditions under comparable irradiance (89.8 ± 24.6 W m^{-2}), achieved 0.48 g L^{-1} d^{-1}, accompanied by high N–NO_3 uptake (28.8 mg L^{-1} d^{-1}) resulting from high nutrient inflow. The subsequent O#12 (Trial #3) recorded a productivity 0.43 g L^{-1} d^{-1} over six days under the highest dilution rate (0.4 d^{-1}) and recirculation (87.5%) during summer.

O#13 employed the same SRT–HRT_{fresh} decoupling (2.5 and 20 d, respectively) as O#12, but ran under Finnish autumn conditions (low outdoor irradiance: 25.8 ± 10.7 W m^{-2}, low daytime: 9.1 ± 1.2 h, low outdoor temperature: 8.6 ± 2.4 °C), resulting in the lowest chemostat productivity (0.32 g L^{-1} d^{-1}). Biomass productivities were similarly low in Trial #4 across all modes (Batch: 0.26 g L^{-1} d^{-1}; Chemostat: 0.32 g L^{-1} d^{-1}; Turbidostat: 0.30 g L^{-1} d^{-1}). In Trial #5, O#9 operated for 20 days with fluctuating outdoor irradiance (17.5–106.1 W m^{-2}) and SRT-HRT configuration as O#7 (5 and 20 d), achieved 0.58 g L^{-1} d^{-1}. While O#7 and O#9 were conducted during comparable spring periods (19 April–15 May 2024, and 15 April–5 May 2025, respectively) the outdoor irradiance during O#9 (~69 W m^{-2}) was ~22% lower compared with O#7 (~88 W m^{-2}). This decrease was accompanied by a shorter natural daylight (−5%) and slightly reduced PBR temperatures (−3%). These seasonal differences in ambient conditions help to explain the 14.7% lower biomass productivity recorded for O#9 (0.58 g L^{-1} d^{-1}) compared to O#7 (0.68 g L^{-1} d^{-1}).

Turbidostat operations (O#14–16) aimed to balance high biomass productivity with suitable drainwater treatment performance. The average productivity of the three turbidostat runs (0.43 ± 0.13 g L^{-1} d^{-1}) was 16.8% lower than the chemostat average but the turbidostat mode achieved 91.4% higher average daily N–NO_3 uptake (33.2 ± 8.8 mg L^{-1} d^{-1}) (Supplementary Fig. S2).

The first turbidostat run (O#14) began in autumn (22 October 2024). The in-line OD_{890} setpoint was fixed at 0.9 (Fig. 3a) to compensate for limited irradiance (14.9 ± 7.4 W m^{-2}), short daylight duration (7.5 ± 1.1 h), and low temperatures (4.8 ± 3.3 °C). Conducted for 30 days, O#14 achieved a productivity of 0.30 g L^{-1} d^{-1} with 341.6 L d^{-1} of harvested culture (equivalent to 2.94 d SRT) and DW between 0.8 and 1.2 g L^{-1}. Biomass growth remained comparable to chemostat levels, while higher nutrient inflow enhanced drainwater treatment performance (Section 3.2).

The subsequent turbidostat runs (O#15 and O#16) were operated during the spring-to-summer transition (5–26 May 2025) under high irradiance (93.9 ± 32.5 W m^{-2}) and extended daylight (up to 17.3 h). Drainwater composition was consistent with typical nutrient concentrations (242–287 mg L^{-1} N–NO_3; 24.3–34.4 mg L^{-1} P–PO_4), ensuring sufficient nutrient supply. The high-OD turbidostat (O#16, OD_{890} = 1.6) was ran for 10 days, yielding 0.55 g L^{-1} d^{-1} -the highest turbidostat productivity (DW between 1.56 and 2.34 g L^{-1}). The average harvested culture volume was 207.6 Ld^{-1}; corresponds to an average actual dilution rate of 0.28 d^{-1} and SRT of 3.57 d.

The reduced harvesting frequency observed in O#16 was defined by the two constraints. Firstly, maintaining a high OD setpoint requires less frequent harvesting. However, this rate was further exacerbated by a technical limitation. The OD sensor operating near its saturation limit diminished sensor's ability to precisely detect the minor density increases, thereby reducing the harvesting cycles. Despite this shift toward a higher biomass concentration than the setpoint, the system reached a maximum sustainable biomass density. The stability and fitness of the culture at this elevated density were supported by the DO profiles (Fig. 3c), which maintained robust diurnal fluctuations throughout O#16. The findings demonstrate that even with sensor saturation and high biomass density, photosynthetic activity remained high and was not significantly inhibited by self-shading. This operational state maximized the biomass productivity under the minimum possible nutrient supply rate with avoiding nutrient stress; thereby promoted biomass-oriented phycoremediation performance characterized by high biomass productivity with efficient use of the limited daily drainwater inflow.

To assess the effect of increased harvesting frequency, the OD_{890} setpoint was lowered to 1.2 in O#15, increasing light and nutrient availability. Operated for 11 days, O#15 reached the highest actual dilution rate of this study (0.45 d^{-1}; 334.3 Ld^{-1} harvested; 75.1% recirculation). Lowering the OD resulted in daily biomass productivity of 0.45 g L^{-1} d^{-1}, which was 18.1% lower than O#16. The mean DW of harvested culture in O#16 (1.72 g L^{-1}) was more than twice in O#15 (0.84 g L^{-1}).

Overall, continuous operations achieved biomass productivities up to 0.68 g L^{-1} d^{-1}. The chemostat mode, with controlled nutrient inflow, provided maximum biomass growth with single daily harvesting, whereas turbidostat mode offered a fine-tuned balance between biomass productivity and drainwater treatment capacity depending on the OD setpoint selected. A total of 81.76 kg of algal biomass was generated over 192 operation days, successfully utilizing high nitrogen loaded drainwater where achieving regulatory discharge compliance is typically difficult.

3.4. Overall system performance and discharge compliance

Of the eleven continuous operations, eight consistently maintained EU-compliant permeate quality, whereas three operations (O#8,10,14) exhibited periods of non-compliance (Table 2). Toward the end of O#8 and O#10, microscopic examinations revealed the invasive phototrophic species outcompeted in the primary culture (Fig. 6b). These operations coincided with peak summer conditions characterized by high outdoor irradiance (83–89 W m^{-2}), elevated outdoor temperatures (25.5–27.2 °C), and extended daylight (15.8–18.2 h), which likely resulted in a breach in biological containment by promoting the proliferation of domestic opportunistic taxa. Consequently, Trials #2 and #3 were terminated early. In O#10, the hydraulic configuration (2.5 d SRT, 5 d HRT) resulted in a high daily N–NO_3 inflow (≈65 mg L^{-1} d^{-1}), demonstrating that short retention times were insufficient for treating drainwaters with elevated nutrient concentrations. In contrast, O#14, conducted during the autumn–winter period, failed to achieve stable removal, with permeate nitrate levels exceeding 50 mg L^{-1}.

Under the scope of maintaining EU-compliant permeate, hydraulic parameters significantly influenced biomass productivity (P_x) and N–NO_3 uptake (r_{N-NO3}). Operations employing longer biomass retention tended to support higher biomass productivity. SRT values exceeding 3 days supported peak productivities, of 0.55 g L^{-1} d^{-1} (O#16) and 0.59 g L^{-1} d^{-1} (O#11) (Fig. 4b). In contrast, operations run at 2.5 d SRT resulted in lower productivities, specifically 0.43 g L^{-1} d^{-1} in O#12 and 0.32 g L^{-1} d^{-1} in O#13 (Fig. 4b). Notably, higher SRT correlated with lower N–NO_3 uptake rates. For example, O#7 and O#9 operating at 5 d SRT showed N–NO_3 uptake rates of 7.1–17.9 mg L^{-1} d^{-1}, while shorter retention times in O#13 and O#14 reached 20.8 and 41.1 mg L^{-1} d^{-1}, respectively (Fig. 4a). HRT further shaped drainwater treatment performance; as shorter HRTs (O#15 and O#14) increased nutrient availability and supported higher daily N–NO_3 uptake (26.1 and 41.1 mg L^{-1} d^{-1}), while longer HRTs (20 d) restricted uptake below 21 mg L^{-1} d^{-1} (Fig. 4a). These modest correlations suggest that hydraulic effects were often confounded by fluctuating outdoor irradiance and variable drainwater composition across operations.

Patterns driven by meteorological conditions were also evaluated to understand the impact of outdoor irradiance and temperature on biomass productivity and N–NO_3 uptake during continuous operations. Higher outdoor irradiance (LI_{mean} and LI_{max}) demonstrated a significant

positive correlation with biomass productivity (P_x) (Fig. 5), which reached peak values of 0.68 g L^{-1} d^{-1} in O#7 and 0.59 g L^{-1} d^{-1} in O#11. In contrast, daily N–NO_3 uptake showed a weak inverse trend under high-irradiance, indicating that nutrient availability, rather than light supply, served as the dominant driver of N–NO_3 uptake (Fig. 3b). This divergence supported a temporal decoupling between biomass growth and nutrient uptake (Fig. 4c). Light availability stimulated biomass formation more strongly than it supported daily N–NO_3 uptake under the specific hydraulic, meteorological, and drainwater characteristics of this study.

Outdoor temperature tracked irradiance closely during the operations (Fig. 5). Because compartment temperature was controlled, the apparent temperature effects largely reflected changes in light availability rather than independent thermal influences. Furthermore, DO showed no significant association with biomass productivity or nutrient uptake under constant aeration (Fig. 5). Together, these outcomes suggest that meteorological drivers influenced biomass formation more directly than N–NO_3 removal, while both processes still operated within the constraints of maintaining EU-compliant permeate.

3.5. Benefits, pitfalls and lessons learned

Benefits. Long-term feasibility and operational stability of continuous phycoremediation were demonstrated under the highly fluctuating conditions typical of Nordic greenhouse operations. Chemostat and turbidostat cultivations were maintained for extended periods across contrasting meteorological regimes, ranging low irradiance phases (<20 W m^{-2} daily mean) to high light conditions (>100 W m^{-2}), while treating drainwater with high nutrient loads (200–420 mg N–NO_3 L^{-1}). Stable biomass production and drainwater treatment were maintained across a broad culture temperature range of 17–37 °C, indicating that *Scenedesmus* sp. NIVA CHL-99 remained physiologically robust within the applied operational parameters. This robustness was established through optimized physicochemical control, including temperature, pH, light supplementation, and hydraulic settings tailored to sustained culture performance. Feedback-regulated control of biomass and nutrient concentrations enabled stable operation under fluctuating influent characteristics without washout or progressive performance decline. Collectively, these results demonstrate that continuous phycoremediation can remain operationally stable across seasonally dynamic greenhouse conditions when environmental control and nutrient uptake kinetics are properly aligned.

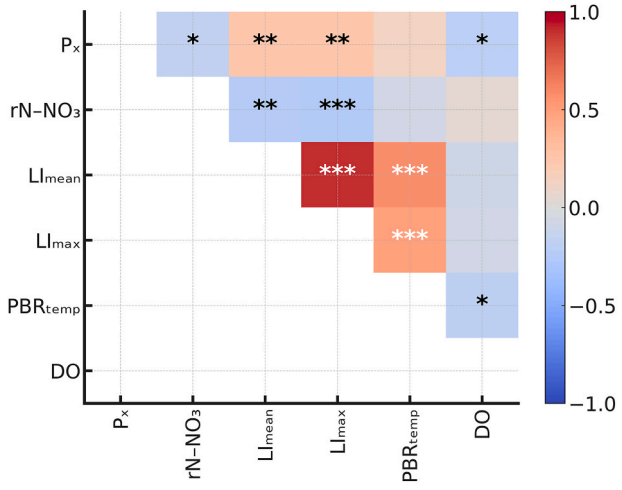

Fig. 5. Pairwise Pearson correlations among process variables, including biomass productivity (P_x), daily nitrate uptake (rN–NO_3), outdoor irradiance (LI_{mean} and LI_{max}), PBR temperature (PBR_{temp}), and dissolved oxygen (DO). Correlation coefficients (r) range from +1 (perfect positive linear relationship) to −1 (perfect negative linear relationship), with significance levels indicated as $p < 0.05$ (*), $p < 0.01$ (**), and $p < 0.001$ (***). Sample sizes varied across variable pairs (n = 143–198).

High drainwater treatment capacity (>25 mg N–NO_3 L^{-1} d^{-1}) was achieved in turbidostat mode while delivering N and P-depleted permeate that met stringent EU discharge limits (Fig. 3b). This outcome carries clear environmental relevance, as N and P losses from agricultural wastewater remain central drivers of eutrophication and coastal water quality decline on a global scale, with agriculture accounting for most diffuse nutrient emissions across Europe (Jwaideh et al., 2022). Nutrient removal was coupled to controlled recycling via algal assimilation, limiting direct nutrient discharge. The algal biomass generated during treatment can serve as a bioagricultural input, with recent studies reporting biostimulant and biopesticidal effects in horticultural applications (Chiaiese et al., 2018; Alling et al., 2023; Jokel et al., 2023). The economic viability of this waste-to-value framework is supported by a growing market demand for these products, with the European biostimulant sector already represents a multibillion-euro market, driven by policies limiting synthetic fertilizer use (EBIC, 2021). The integration of phycoremediation within greenhouse operations supports a circular greenhouse–wastewater–biomass approach suitable for nutrient management in Northern European greenhouse systems.

Challenges. Strong seasonal asymmetry in light availability emerged as a defining constraint for the process. In this study, daily average outdoor irradiance during autumn–winter periods declined by 85–90% compared to spring–summer conditions (15 W m^{-2} versus 118 W m^{-2}), directly reducing biomass productivity (Table 1). Maintaining continuous operation under these low-irradiance conditions required increased reliance on artificial lighting and greenhouse heating, rendering the process increasingly energy-intensive. While Finnish greenhouse production has been reported to require approximately two to three times higher heat demand in winter (Kaukoranta et al., 2017; Kumar et al., 2022), from an integrated greenhouse perspective, these winter energy inputs could transform this seasonal challenge into an opportunity by supporting parallel microalgal cultivation through shared use of existing heat and electricity infrastructure.

At the opposite seasonal extreme, summer operations in this study were constrained by elevated biotic stress within the greenhouse. Higher temperatures combined with nutrient-rich media promoted contamination by non-target organisms, shortening several trials and reducing culture consistency (Fig. 6b). Contamination is widely recognized as a major limitation in large-scale microalgae cultivation, as warm conditions accelerate the proliferation of competing algae, grazers, and associated microbial communities (Molina-Grima et al., 2022; Novoveská et al., 2023). Beyond operational stability, contamination directly affects biomass quality and limits its suitability for downstream valorization, thereby reducing industrial relevance (Zhu et al., 2020).

Performance-compliance trade-offs became evident when operating with nutrient-rich drainwater. As expected, increasing nutrient inflow rates enhanced daily nutrient removal, aligning with the primary objective of maximizing drainwater treatment capacity. However, maintaining EU-compliant discharge proved increasingly difficult as treatment intensity increased. Because the recirculation fraction was fixed, residual nitrogen or phosphorus in the permeate re-entered PBR, increasing the effective daily nutrient input through a positive feedback mechanism (Trial#4 case). This sensitive dependency underscores a key environmental sustainability trade-off, where intensifying nutrient removal must be reconciled with discharge quality and broader ecological impacts (Discart et al., 2014; Wik et al., 2020).

Insights. Nutrient recycling without biomass retention enabled continuous exposure of the culture to nutrient-rich drainwater while maintaining operational continuity, indicating that decoupled HRT-SRT is a relevant consideration for realistic large-scale phycoremediation. Within this configuration, turbidostat operation proved particularly meaningful for industrial applications because it allows active regulation of biomass concentration under fluctuating growth conditions. However, this benefit comes with increased technical demand, as

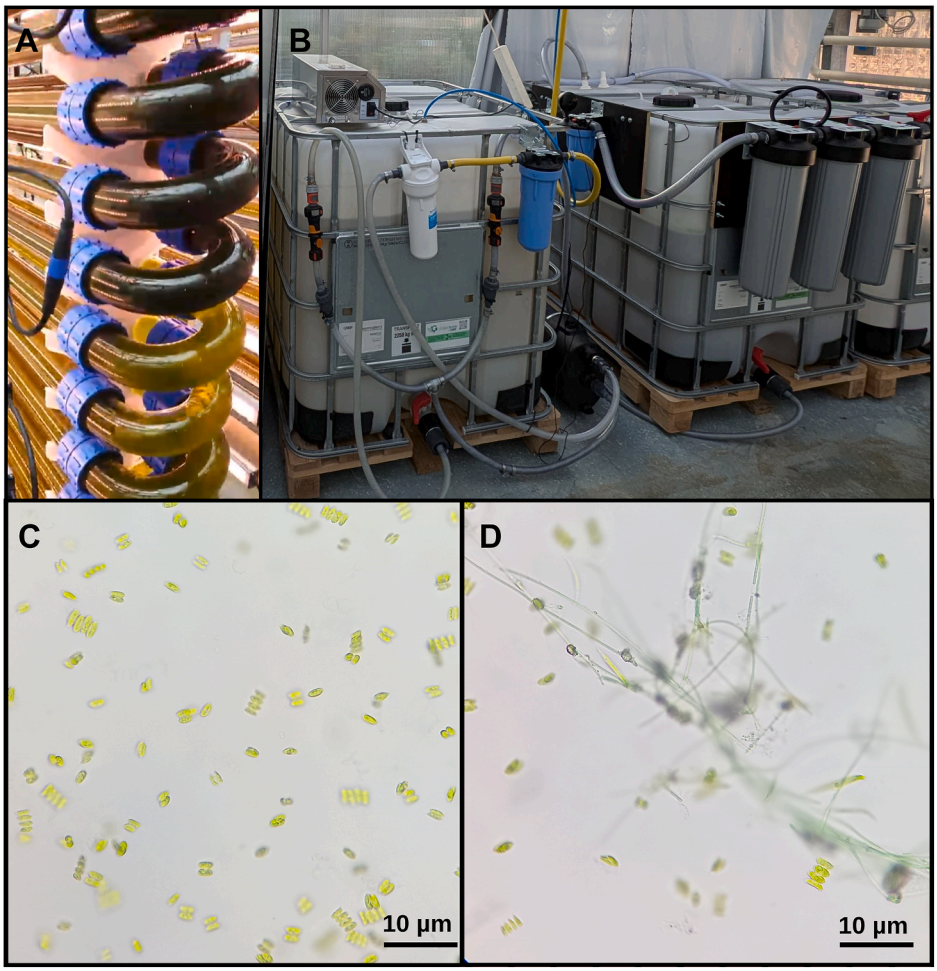

Fig. 6. Challenges affecting the operational stability of large-scale phycoremediation. **(a)** Chemical sedimentation and mineral precipitation, **(b)** nutrient mismanagement resulting from technical sensor limitations, **(c)** primary culture *Scenedesmus* sp. NIVA CHL-99 and **(d)** contamination with opportunistic taxa.

turbidostat control relies on accurate sensing, responsive control loops, and tight integration between biomass regulation and nutrient management (O#16 case). The results therefore suggest that widespread implementation may be constrained if system complexity outweighs operational simplicity (Fig. 6c). Hybrid phycoremediation strategies that retain the adaptive advantages of turbidostat control while simplifying implementation may offer a more practical balance between controllability and scalability for greenhouse-based applications.

Static operational settings constrained system performance under the variable Nordic environmental conditions encountered in this long-term study. Improving responsiveness to hydraulic and meteorological variability is therefore essential to remain sustainable and efficient at large-scale treatment. Machine learning–based and adaptive control strategies are well suited for this purpose, as they enable dynamic adjustment of lighting, heating, and operational setpoints based on real-time system behavior (Caparroz et al., 2024). Dynamic approaches, supported by high-sensitivity in-line monitoring, could regulate daily nutrient inflow and maintain discharge compliance under multi-parameter variability (Fig. 6c). In this context, real-time monitoring may enable targeted adjustment of nutrient stoichiometry to counteract the temporal decoupling of N and P uptake, providing a potential route to enhance drainwater treatment capacity.

4. Conclusions

Continuous phycoremediation represents a robust algae-based solution for treating nutrient-rich agricultural drainwater under the seasonally dynamic conditions of Nordic greenhouses. Long-term pilot-scale operation confirmed that both chemostat and turbidostat strategies can consistently achieve EU-compliant nitrogen and phosphorus discharge while maintaining stable performance under fluctuating light, temperature, and influent nutrient loads.

Turbidostat operation revealed a clear trade-off between nutrient removal performance and biomass productivity performance during phycoremediation. Biomass productivity was maximized under high-density control (up to 0.55 g L^{-1} d^{-1}), whereas $N–NO_3$ removal peaked during low-density operation (up to 41 mg $N–NO_3$ L^{-1} d^{-1}), indicating that nitrogen-limited permeate conditions are required to prevent residual nitrate in the final discharge. Furthermore, temporal decoupling between nitrate and phosphate uptake limits the reliability of static nutrient inflow control for protecting discharge quality. This constraint highlights the need for adaptive nutrient dosing and real-time stoichiometric monitoring for achieving environmentally sound scale-up.

This study demonstrates one of the first pilot-scale implementations of turbidostat phycoremediation under seasonally variable greenhouse conditions. Stable operation enabled regulatory-compliant drainwater treatment alongside sustained biomass productivity and nutrient recovery. By transforming greenhouse drainwater into a valuable resource, this integrated approach reduces reliance on external fertilizers and freshwater, thereby improving the economic viability of microalgal cultivation. Collectively, continuous phycoremediation represents a practical and scalable pathway toward cost-efficient horticultural wastewater management within a circular bioeconomy framework.

CRediT authorship contribution statement

Emren Borhan: Writing – original draft, Visualization, Validation, Methodology, Investigation, Formal analysis, Data curation, Conceptualization. **Ville Korhonen:** Investigation, Data curation. **Sema Sirin:** Writing – review & editing, Validation, Supervision, Project administration, Methodology, Conceptualization. **Yagut Allahverdiyeva:** Writing – review & editing, Supervision, Project administration, Funding acquisition, Conceptualization.

Declaration of generative AI use in the writing process

During manuscript preparation, ChatGPT was used to assist with language and readability. The authors reviewed and edited all outputs as necessary and take full responsibility for the final published content.

Funding

This research was funded by the European Union (Grant agreement ID: 101060991, REALM), a donation from Maa-ja vesitekniikan tuki ry, University of Turku Graduate School (UTUGS), and Business Finland Co-Research AlgaCircle (Project number: 2621/31/2024). The authors also acknowledge the FIN-BioFoundry FIRI infrastructure for providing technical background and facilities.

Declaration of competing interest

The authors declare that they have no known competing financial interests or personal relationships that could have appeared to influence the work reported in this paper.

Acknowledgements

The authors acknowledge Tapio Ronkainen and the staff of the Ruissalo Botanical Garden for their technical support during greenhouse operations. We thank Timo Juntti for granting access to hydroponic drainwater and for facilitating its transport, and to Scigrafik (Dmitry Shevela) for the graphical abstract.

Appendix A. Supplementary data

Supplementary data to this article can be found online at https://doi.org/10.1016/j.jenvman.2026.129635.

Data availability

Data will be made available on request.

References

Abdelfattah, A., Ali, S.S., Ramadan, H., El-Aswar, E.I., Eltawab, R., Ho, S.-H., Elsamahy, T., Li, S., El-Sheekh, M.M., Schagerl, M., Kornaros, M., Sun, J., 2023. Microalgae-based wastewater treatment: mechanisms, challenges, recent advances, and future prospects. Environ. Sci. Ecotechnol. 13, 100205. https://doi.org/10.1016/j.ese.2022.100205.

Alling, T., Funk, C., Gentili, F.G., 2023. Nordic microalgae produce biostimulant for the germination of tomato and barley seeds. Sci. Rep. 13 (1), 3509. https://doi.org/10.1038/s41598-023-30707-8.

Álvarez-Gil, M., Blanco-Vieites, M., Suárez-Montes, D., Casado-Bañares, V., Delgado-Ramallo, J.F., Rodríguez, E., 2023. Revolutionizing agriculture: leveraging hydroponic greenhouse wastewater for sustainable microalgae-based biostimulant production. Sustainability 15 (19), 14398. https://doi.org/10.3390/su151914398.

Amaro, H.M., Salgado, E.M., Nunes, O.C., Pires, J.C.M., Esteves, A.F., 2023. Microalgae systems – environmental agents for wastewater treatment and further potential biomass valorisation. J. Environ. Manag. 337, 117678. https://doi.org/10.1016/j.jenvman.2023.117678.

American Public Health Association, American Water Works Association, Water Environment Federation. Standard Methods for the Examination of Water and Wastewater. eighteenth ed. Section 4500-NO_3-B: Ultraviolet Spectrophotometric Screening Method for Nitrate.

Aparicio, S., Borrás-Falomir, L., Jiménez-Benítez, A., Seco, A., Robles, Á., 2024. Urban wastewater treatment at ambient conditions using microalgae-bacteria consortia in a membrane high-rate algal pond (MHRAP): the effect of hydraulic retention time and influent strength. Environ. Technol. Innovat. 36, 103846. https://doi.org/10.1016/j.eti.2024.103846.

Arashiro, L.T., Josa i Culleré, I., Ferrer Martí, I., van Hulle, S., Rousseau, D.P.L., Garfí, M., 2022. Life cycle assessment of microalgae systems for wastewater treatment and bioproducts recovery: natural pigments, biofertilizer and biogas. Sci. Total Environ. 847, 157615. https://doi.org/10.1016/j.scitotenv.2022.157615.

Barbera, E., Sforza, E., Grandi, A., Bertucco, A., 2020. Uncoupling solid and hydraulic retention time in photobioreactors for microalgae mass production: a model-based analysis. Chem. Eng. Sci. 218, 115578. https://doi.org/10.1016/j.ces.2020.115578.

Benke, K., Tomkins, B., 2017. Future food-production systems: vertical farming and controlled-environment agriculture. Sustain. Sci. Pract. Pol. 13 (1), 13–26. https://doi.org/10.1080/15487733.2017.1394054.

Caparroz, M., Guzmán, J.L., Berenguel, M., Acién, F.G., 2024. A novel data-driven model for prediction and adaptive control of pH in raceway reactor for microalgae cultivation. N. Biotech. 82, 1–13. https://doi.org/10.1016/j.nbt.2024.04.001.

Carpenter, S.R., Caraco, N.F., Correll, D.L., Howarth, R.W., Sharpley, A.N., Smith, V.H., 1998. Nonpoint pollution of surface waters with phosphorus and nitrogen. Ecol. Appl. 8 (3), 559–568. https://doi.org/10.1890/1051-0761(1998)008[0559:NPOSWW]2.0.CO;2.

Chathurika, G.L., Bandara, L., Abeysiriwardana-Arachchige, I.S.A., Xu, X., Lin, L., Jiang, W., Zhang, Y., Johnson, D.C., Nirmalakhandan, N., Xu, P., 2022. Impacts of seasonality and operating conditions on water quality of algal versus conventional wastewater treatment: part 1. J. Environ. Manag. 304, 114291. https://doi.org/10.1016/j.jenvman.2021.114291.

Chiaiese, P., Corrado, G., Colla, G., Kyriacou, M.C., Rouphael, Y., 2018. Renewable sources of plant biostimulation: microalgae as a sustainable means to improve crop performance. Front. Plant Sci. 9, 1782. https://doi.org/10.3389/fpls.2018.01782.

Ciardi, M., Gómez-Serrano, C., Morales-Amaral, M.M., Acién, G., Lafarga, T., Fernández-Sevilla, J.M., 2022. Optimisation of *Scenedesmus almeriensis* production using pig slurry as the sole nutrient source. Algal Res. 61, 102580. https://doi.org/10.1016/j.algal.2021.102580.

Discart, V., Bilad, M.R., Marbelia, L., Vankelecom, I.F.J., 2014. Impact of changes in broth composition on *Chlorella vulgaris* cultivation in a membrane photobioreactor (MPBR) with permeate recycle. Bioresour. Technol. 152, 321–328. https://doi.org/10.1016/j.biortech.2013.11.019.

Díez-Montero, R., Bělohlav, V., Ortiz, A., Uggetti, E., García-Galán, M.J., García, J., 2020. Evaluation of daily and seasonal variations in a semi-closed photobioreactor for microalgae-based bioremediation of agricultural runoff at full-scale. Algal Res. 47, 101859. https://doi.org/10.1016/j.algal.2020.101859.

European Biostimulants Industry Council. Market overview. biostimulants.eu. https://biostimulants.eu/plant-biostimulants/market-overview/.

European Commission, 2020a. *The European Green Deal*. COM (2019) 640 final. https://eur-lex.europa.eu/legal-content/EN/TXT/?uri=CELEX:52019DC0640.

European Commission, 2020b. A New Circular Economy Action Plan for a Cleaner and More Competitive Europe. COM. https://eur-lex.europa.eu/legal-content/EN/TXT/?uri=CELEX:52020DC0098.

European Commission, 2022. *Towards a strong and sustainable EU algae sector*. COM (2022) 592 final. https://eur-lex.europa.eu/legalcontent/EN/TXT/?uri=CELEX:52022DC0592.

Geng, Y., Shaukat, A., Azhar, W., Raza, Q.-U.-A., Tahir, A., Zain-ul-Abideen, M., Rehim, A., 2025. Microalgal biorefineries: technological trade-offs and innovation pathways. Biotechnol. Biofuels Bioprod. 18, 93. https://doi.org/10.1186/s13068-025-02694-7.

Goh, P.S., Ahmad, N.A., Lim, J.W., Liang, Y.Y., Kang, H.S., Ismail, A.F., Arthanareeswaran, G., 2022. Microalgae-enabled wastewater remediation and nutrient recovery through membrane photobioreactors: recent achievements and future perspective. Membranes 12 (11), 1094. https://doi.org/10.3390/membranes12111094.

Gonçalves, A.L., Simões, M., Pires, J.C.M., 2014. The effect of light supply on microalgal growth, CO_2 uptake and nutrient removal from wastewater. Energy Convers. Manag. 85, 530–536. https://doi.org/10.1016/j.enconman.2014.05.085.

Grewal, H.S., Maheshwari, B., Parks, S.E., 2011. Water and nutrient use efficiency of a low-cost hydroponic greenhouse for a cucumber crop: an Australian case study. Agric. Water Manag. 98 (5), 841–846. https://doi.org/10.1016/j.agwat.2010.12.010.

Halleux, V., 2024. *Urban Wastewater Treatment: Updating EU Rules* (EU Legislation in Progress Briefing, PE 739.370). European Parliamentary Research Service, European Parliament. https://www.europarl.europa.eu/RegData/etudes/BRIE/2023/739370/EPRS_BRI(2023)739370_EN.pdf.

Hultberg, M., Carlsson, A.S., Gustafsson, S., 2013. Treatment of drainage solution from hydroponic greenhouse production with microalgae. Bioresour. Technol. 136, 401–406. https://doi.org/10.1016/j.biortech.2013.03.019.

Jokel, M., Salazar, J., Chovancek, E., Sirin, S., Allahverdiyeva, Y., 2023. Screening of several microalgae revealed biopesticide properties of *Chlorella sorokiniana* against the strawberry pathogen *Phytophthora cactorum*. J. Appl. Phycol. 35 (6), 2675–2687. https://doi.org/10.1007/s10811-023-03015-x.

Juncal, M.J.L., Masino, P., Bertone, E., Stewart, R.A., 2023. Towards nutrient neutrality: a review of agricultural runoff mitigation strategies and the development of a decision-making framework. Sci. Total Environ. 874, 162408. https://doi.org/10.1016/j.scitotenv.2023.162408.

Jwaideh, M.A.A., Sutanudjaja, E.H., Dalin, C., 2022. Global impacts of nitrogen and phosphorus fertiliser use for major crops on aquatic biodiversity. Int. J. Life Cycle Assess. 27 (8), 1058–1080. https://doi.org/10.1007/s11367-022-02078-1.

Katzin, D., Marcelis, L.F.M., van Mourik, S., 2021. Energy savings in greenhouses by transition from high-pressure sodium to LED lighting. Appl. Energy 281, 116019. https://doi.org/10.1016/j.apenergy.2020.116019.

Kaukoranta, T., Särkkä, L.E., Jokinen, K., 2017. Energy efficiency of greenhouse cucumber production under LED and HPS lighting. Acta Hortic. 1170, 967–972. https://doi.org/10.17660/ActaHortic.2017.1170.124.

Konkol, I., Kuligowski, K., Szafranowicz, P., Vorne, V., Reinikainen, A., Effelsberg, N., Christensen, M.L., Svensson, M., Zviedris, J., Dvarioniene, J., Cenian, A., 2024. Review of the seasonal wastewater challenges in Baltic coastal tourist areas: insights from the NURSECOAST-II project. Sustainability 16 (22), 9890. https://doi.org/10.3390/su16229890.

Kotai, J., 1972. Instructions for Preparation of Modified Nutrient Solution Z8 for Algae. Norwegian Institute for Water Research. Report No. 11/69, 5.

Kumar, M., Haillot, D., Gibout, S., 2022. Survey and evaluation of solar technologies for agricultural greenhouse application. Sol. Energy 232, 18–34. https://doi.org/10.1016/j.solener.2021.12.033.

Li, K., Liu, Q., Fang, F., Luo, R., Lu, Q., Zhou, W., Huo, S., Cheng, P., Liu, J., Addy, M., Chen, P., Chen, D., Ruan, R., 2019. Microalgae-based wastewater treatment for nutrients recovery: a review. Bioresour. Technol. 291, 121934. https://doi.org/10.1016/j.biortech.2019.121934.

Liu, J., Wang, H., Peñuelas, J., Mou, J., Delgado-Baquerizo, M., Sardans, J., Coello, F., Quan, Z., Qiu, T., Li, Y., Guo, Y., Hu, Z., Ying, Y., Lv, J., Zhang, Y., Tan, W., Zhou, G., Li, L.-J., Fang, L., 2025. Global nitrogen and phosphorus use efficiencies and nutrient budgets: a synthesis of large-scale patterns and drivers. Nat. Commun. 16, 66019. https://doi.org/10.1038/s41467-025-66019-w.

Marttila, M.P., Uusitalo, V., Linnanen, L., Mikkilä, M.H., 2021. Agro-industrial symbiosis and alternative heating systems for decreasing the global warming potential of greenhouse production. Sustainability 13 (16), 9040. https://doi.org/10.3390/su13169040.

Masojídek, J., Štěrbová, K., Robles Carnero, V.A., Torzillo, G., Gómez-Serrano, C., Cicchi, B., Câmara Manoel, J.A., Silva Benavides, A.M., Barceló-Villalobos, M., Pozo Dengra, J., 2024. Photosynthetic activity measured *in situ* in microalgae cultures grown in pilot-scale raceway ponds. Plants 13 (23), 3376. https://doi.org/10.3390/plants13233376.

Mercado, I., Álvarez, X., Verduga, M.-E., Cruz, A., 2020. Enhancement of biomass and lipid productivities of *Scenedesmus* sp. cultivated in the wastewater of the dairy industry. Processes 8 (11), 1458. https://doi.org/10.3390/pr8111458.

Mielcarek, A., Kłobukowska, K., Rodziewicz, J., Janczukowicz, W., Bryszewski, K.Ł., 2024. Advanced treatment of nutrient-rich effluents using decentralized systems. Sustainability 16 (1), 152. https://doi.org/10.3390/su16010152.

Ministry of Climate and Environment, 2024. Meld. St. 35 (2023–2024): *Sustainable use and conservation of biodiversity*. Government of Norway. https://www.regjeringen.no/en/documents/meld.-st.-35-20232024/id3054780/.

Ministry of the Environment, Finnish Environment Institute, Ministry of Agriculture and Forestry of Finland, Ministry of Transport and Communications, & Centre of Economic Development, Transport and Environment, 2023. Towards a good state of the Baltic Sea: programme of measures of Finland's Marine Strategy 2022–2027 in a nutshell. https://www.doria.fi/handle/10024/188643.

Mohsenpour, S.F., Hennige, S., Willoughby, N., Adeloye, A.J., Gutierrez, T., 2021. Integrating micro-algae into wastewater treatment: a review. Sci. Total Environ. 752, 142168. https://doi.org/10.1016/j.scitotenv.2020.142168.

Molina-Grima, E., García-Camacho, F., Acién-Fernández, F.G., Sánchez-Mirón, A., Plouviez, M., Shene, C., Chisti, Y., 2022. Pathogens and predators impacting commercial production of microalgae and Cyanobacteria. Biotechnol. Adv. 55, 107884. https://doi.org/10.1016/j.biotechadv.2021.107884.

Morillas-España, A., Pérez-Crespo, R., Villaró-Cos, S., Rodríguez-Chikri, L., Lafarga, T., 2024. Integrating microalgae-based wastewater treatment, biostimulant production, and hydroponic cultivation: a sustainable approach to water management and crop production. Front. Bioeng. Biotechnol. 12, 1364490. https://doi.org/10.3389/fbioe.2024.1364490.

Nagarajan, D., Lee, D.-J., Chen, C.-Y., Chang, J.-S., 2020. Resource recovery from wastewaters using microalgae-based approaches. Bioresour. Technol. 302, 122817. https://doi.org/10.1016/j.biortech.2020.122817.

Najar-Almanzor, J.E., González-Delgado, Á.D., Kafarov, V., 2023. Microalgae-assisted green bioremediation of food-processing wastewater: a sustainable approach toward a circular economy concept. J. Environ. Manag. 345, 118774. https://doi.org/10.1016/j.jenvman.2023.118774.

Nguyen, L.N., Aditya, L., Vu, H.P., Johir, A.H., Bennar, L., Ralph, P., Hoang, N.B., Zdarta, J., Nghiem, L.D., 2022. Microalgae-based wastewater treatment for nutrients removal: current status and future perspectives. Environ. Chem. Lett. 20, 1623–1649. https://doi.org/10.1007/s40726-022-00230-x.

Nordio, R., Belachqer-El Attar, S., Clagnan, E., Sánchez-Zurano, A., Pichel, N., Viviano, E., Adani, F., Guzmán, J.L., Acién, G., 2024. Exploring microbial growth dynamics in a pilot-scale microalgae raceway fed with urban wastewater: insights into the effect of operational variables. J. Environ. Manag. 369, 122385. https://doi.org/10.1016/j.jenvman.2024.122385.

Novoveská, L., Nielsen, S.L., Eroldoğan, O.T., Haznedaroglu, B.Z., Rinkevich, B., Fazi, S., Robbens, J., Vasquez, M., Einarsson, H., 2023. Overview and challenges of large-scale cultivation of photosynthetic microalgae and Cyanobacteria. Mar. Drugs 21 (8), 445. https://doi.org/10.3390/md21080445.

OECD, 2025. Agricultural Policy Monitoring and Evaluation 2025: Making the Most of the Trade and Environment Nexus in Agriculture. OECD Publishing, Paris. https://doi.org/10.1787/a80ac398-en.

Park, J.B.K., Craggs, R.J., Shilton, A.N., 2011. Wastewater treatment high-rate algal ponds. Bioresour. Technol. 102, 35–42. https://doi.org/10.1016/j.biortech.2010.06.158.

Pataro, I.M.L., Gil, J.D., Guzmán, J.L., Berenguel, M., Lemos, J.M., 2023. Learning-based model predictive strategy for pH control in photobioreactors. Control Eng. Pract. 138, 105619. https://doi.org/10.1016/j.conengprac.2023.105619.

Preisner, M., Neverova-Dziopak, E., Kowalewski, Z., 2020. An analytical review of different approaches to wastewater discharge standards with particular emphasis on nutrients. Environ. Manag. 66, 694–708. https://doi.org/10.1007/s00267-020-01344-y.

Rani, V., Maróti, G., 2023. Light-dependent nitrate removal capacity of green microalgae. Int. J. Mol. Sci. 24 (1), 77. https://doi.org/10.3390/ijms24010077.

Salazar, J., Santana-Sánchez, A., Näkkilä, J., Sirin, S., Allahverdiyeva, Y., 2023. Complete N and P removal from hydroponic greenhouse wastewater by *Tetradesmus obliquus*: a strategy for algal bioremediation and cultivation in Nordic countries. Algal Res. 70, 102988. https://doi.org/10.1016/j.algal.2023.102988.

Salazar, J., Valev, D., Näkkilä, J., Tyystjärvi, E., Sirin, S., Allahverdiyeva, Y., 2021. Nutrient removal from hydroponic effluent by Nordic microalgae: from screening to a greenhouse photobioreactor operation. Algal Res. 55, 102247. https://doi.org/10.1016/j.algal.2021.102247.

Sánchez-Contreras, M.I., Morales-Arrieta, S., Okoye, P.U., Guillén-Garcés, R.A., Sebastian, P.J., Arias, D.M., 2021. Recycling industrial wastewater for improved carbohydrate-rich biomass production in a semi-continuous photobioreactor: effect of hydraulic retention time. J. Environ. Manag. 284, 112065. https://doi.org/10.1016/j.jenvman.2021.112065.

Shayesteh, H., Vadiveloo, A., Bahri, P.A., Moheimani, N.R., 2022. Long term outdoor microalgal phycoremediation of anaerobically digested abattoir effluent. J. Environ. Manag. 323, 116322. https://doi.org/10.1016/j.jenvman.2022.116322.

Silambarasan, S., Logeswari, P., Sivaramakrishnan, R., Incharoensakdi, A., Kamaraj, B., Cornejo, P., 2023. *Scenedesmus* sp. strain SD07 cultivation in municipal wastewater for pollutant removal and production of lipid and exopolysaccharides. Environ. Res. 218, 115051. https://doi.org/10.1016/j.envres.2022.115051.

Sutherland, D.L., Heubeck, S., Park, J., Turnbull, M.H., Craggs, R.J., 2018. Seasonal performance of a full-scale wastewater treatment enhanced pond system. Water Res. 136, 150–159. https://doi.org/10.1016/j.watres.2018.02.046.

Solovchenko, A., Khozin-Goldberg, I., Selyakh, I., Semenova, L., Ismagulova, T., Lukyanov, A., Mamedov, I., Vinogradova, E., Karpova, O., Konyukhov, I., Vasilieva, S., Mojzes, P., Dijkema, C., Vecherskaya, M., Zvyagin, I., Nedbal, L., Gorelova, O., 2019. Phosphorus starvation and luxury uptake in green microalgae revisited. Algal Res. 43, 101651. https://doi.org/10.1016/j.algal.2019.101651.

Tong, X., Zhang, X., Fensholt, R., Jensen, P.R.D., Li, S., Larsen, M.N., Reiner, F., Tian, F., Brandt, M., 2024. Global expansion of greenhouse cultivation revealed by satellite mapping. Nat. Food 5, 513–523. https://doi.org/10.1038/s43016-024-00985-0.

Unc, A., Altdorff, D., Abakumov, E., Adl, S., Baldursson, S., Bechtold, M., Cattani, D.J., Firbank, L.G., Grand, S., Guðjónsdóttir, M., Kallenbach, C., Kedir, A.J., Li, P., McKenzie, D.B., Misra, D., Nagano, H., Neher, D.A., Niemi, J., Oelbermann, M., Overgård Lehmann, J., Parsons, D., Quideau, S., Sharkhuu, A., Smreczak, B., Sorvali, J., Vallotton, J.D., Whalen, J.K., Young, E.H., Zhang, M., Borchard, N., 2021. Nordic agriculture under climate change: challenges, opportunities and adaptation strategies for crop production. Front. Sustain. Food Syst. 5, 663448. https://doi.org/10.3389/fsufs.2021.663448.

Valev, D., Silva Santos, H., Tyystjärvi, E., 2020. Stable wastewater treatment with *Neochloris oleoabundans* in a tubular photobioreactor. J. Appl. Phycol. 32 (1), 399–410. https://doi.org/10.1007/s10811-019-01890-x.

Velasco, M.H., 2021. Enabling year-round cultivation in the Nordics: agrivoltaics and adaptive LED lighting control of daily light integral. Agriculture 11 (12), 1255. https://doi.org/10.3390/agriculture11121255.

Velásquez-Orta, S.B., Yáñez-Noguez, I., Monje-Ramírez, I., Orta-Ledesma, M.T., 2024. Pilot-scale microalgae cultivation and wastewater treatment. Environ. Sci. Pollut. Control Ser. 31, 46994–47021. https://doi.org/10.1007/s11356-024-34000-7.

Wacker, J.-D., Verheul, M., Righini, I., Maessen, H., Stanghellini, C., 2022. Optimisation of supplemental light systems in Norwegian tomato greenhouses – a simulation study. Biosyst. Eng. 215, 129–142. https://doi.org/10.1016/j.biosystemseng.2021.12.020.

Wik, B., Rittmann, B.E., Marcus, A.K., 2020. Evaluating the benefits of permeate recycling in a photobioreactor using multi-component, community-level modeling. Algal Res. 51, 102052. https://doi.org/10.1016/j.algal.2020.102052.

Withers, P.J.A., Neal, C., Jarvie, H.P., Doody, D.G., 2014. Agriculture and eutrophication: where do we go from here? Sustainability 6 (9), 5853–5875. https://doi.org/10.3390/su6095853.

Wu, B., Tian, F., Zhang, M., Piao, S., Zeng, H., Zhu, W., Liu, J., Elnashar, A., 2022. Quantifying global agricultural water appropriation with data derived from earth observations. J. Clean. Prod. 358, 131891. https://doi.org/10.1016/j.jclepro.2022.131891.

Xu, Y., Wei, C., Liu, D., Li, J., Tian, B., Li, Z., Xu, L., 2024. Life-cycle and economic assessments of microalgae biogas production in suspension and biofilm cultivation systems. Bioresour. Technol. 395, 130381. https://doi.org/10.1016/j.biortech.2024.130381.

You, X., Yang, L., Zhou, X., Zhang, Y., 2022. Current status and challenges of microalgae-based wastewater treatment: a comprehensive review. Environ. Res. 210, 112860. https://doi.org/10.1016/j.envres.2022.112860.

Zhu, Z., Jiang, J., Fa, Y., 2020. Overcoming the biological contamination in microalgae and Cyanobacteria mass cultivations for photosynthetic biofuel production. Molecules 25 (22), 5220. https://doi.org/10.3390/molecules25225220.